CEMENTITIOUS BARRIERS PARTNERSHIP

X-RAY DIFFRACTION OF SLAG-BASED SODIUM SALT WASTE FORMS

C. A. Langton and D. M. Missimer
Savannah River National Laboratory
Savannah River Site
Aiken, South Carolina 29808

June, 2014

CBP-TR-2014-004, Rev. 0

ACKNOWLEDGEMENTS

This report was prepared for the United States Department of Energy under Interagency Agreement No. DE-AI09-09SR22667 and is an account of work performed under that contract. This report was also prepared with the financial support by the U. S. Department of Energy, under Cooperative Agreement Number DE-FC01-06EW07053 entitled 'The Consortium for Risk Evaluation with Stakeholder Participation III' awarded to Vanderbilt University. Reference herein to any specific commercial product, process, or service by trademark, name, manufacturer, or otherwise does not necessarily constitute or imply endorsement, recommendation, or favoring of same by Savannah River Nuclear Solutions, Vanderbilt University or by the United States Government or any agency thereof. The views and opinions of the authors expressed herein do not necessarily state or reflect those of the United States Government or any agency thereof. This report is part of a larger multi-investigator project supported by the U. S. Department of Energy entitled the Cementitious Barriers Partnership. The opinions, findings, conclusions, or recommendations expressed herein are those of the authors and do not necessarily represent the views of the U.S. Department of Energy. This work was also partially supported by the National Institute of Standards and Technology Sustainable, High Performance Infrastructure Materials program.

DISCLAIMER

Printed in the United States of America
United States Department of Energy
Office of Environmental Management
Washington, DC

SUMMARY

Cementitious materials are used to solidify and stabilize aqueous based radioactive waste containing sodium salts. The types and proportions of cementitious ingredients used to treat aqueous radioactive waste streams containing sodium salts depend on the performance objectives for the waste forms and the compositions of the waste streams. Matrix phases can stabilize certain contaminants (co-precipitation, substitution, ion exchange, and / or sorption), influence processing properties, and are responsible for physical properties and durability of the cured waste forms. Consequently, characterization of the matrix (binder) mineralogy (chemical compositions and crystalline / non crystalline structures) is important for predicting contaminant leaching and evolution of the materials as a function of time and changing conditions

This report documents sample preparation and x-ray diffraction results for a series of mixtures of sodium salt waste and cementitious binders. The objective of this study was to provide initial phase characterization for the CBP reference case cementitious salt waste form. This information can be used to: 1) generate a base line for the evolution of the waste form as a function of time and conditions, 2) potentially to design new binders based on mineralogy of the binder, 3) understand and predict anion and cation leaching behavior of contaminants of concern, and 4) predict performance of the waste forms for which phase solubility and thermodynamic data are available. Characterization of the mineralogy is also important for understanding the buffering effects that the waste form has on infiltrating water / leachates.

More specifically, identification of hydrated phases capable of sequestering anions in the structures and crystallinity of the calcium silicate binder phases were of particular interest. The intent was to use this characterization data as a starting point for more detailed phase characterization using neutron diffraction techniques in addition to quasi-elastic neutron scattering techniques for characterization of water at the ORNL Spallation Neutron Source, Oak Ridge, TN. The initial characterization is complete. Due to extensive substitutions of cations and anions in the layered double hydroxide phases and the very fine intermixing of poorly crystalline hydrated phases in the reference case blend (10 : 45 : 45 cement : slag : fly ash), electron diffraction and transmission electron spectroscopy are recommended as the next step for characterization.

In summary, the hydrated mixtures of Type II portland cement, Grade 100 ground granulated blast furnace slag (GGBFS) and carbon burn-out (CBO) Class F Fly ash contained hydrated phase assemblages which were typical of those reported in the literature. Based on x-ray diffraction results, no significant differences were detected in samples cured 2 months and 14 months in sealed containers at ambient indoor temperatures.

Slag and a blend of slag and cement hydrated with caustic 5 M Na salt solution resulted in the most crystalline matrix. In addition to poorly to non-crystalline C-S-H, these samples contained fairly well ordered C-S-H I (a precursor of 14Å tobermorite) and 11 Å Al-substituted tobermorite. These crystalline C-S-H phases did not form or were present in trace amounts in slag blends containing 30 to 45 mass percent fly ash. The calcium silicate binder in the 10:45:45 mixture of cement : slag : fly ash was primarily non crystalline to poorly crystalline C-S-H. The sample cured for 14 months may contain a small amount of the more crystalline calcium silicate hydrate phases.

Layered double hydroxides in the hydrotalcite (magnesium-aluminum carbonate hydroxide) and hydrocalumite / AFm phases (calcium aluminum hydroxide) were present in mixtures containing slag. The specific phase(s) were not identified because these phases form solid solutions and have a considerable amount of overlap in their x-ray patterns.

Sodium nitrate was the only sodium salt phase identified in x-ray diffraction patterns of the samples hydrated with salt solution. Sodium nitrate is distributed throughout the matrix of samples cured under non-drying conditions as very small crystals which are not obvious in SEM micrographs at magnification of a few 1000X. Drying conditions during curing, especially when coupled with elevated temperatures, result in formation of large sodium nitrate crystals which exhibit a twisted, bundle morphology. These crystals are often associated with localized cracking and a damaged microstructure not observed in samples cured under non-drying conditions.

Sodium sulfate, aluminate, and carbonate were to a large extent incorporated in the structures of the layered double hydroxide (AFm) type phases. These mixed metal layered double hydroxides make up an important fraction of the matrix in the slag containing blends hydrated with caustic salt solution. They are among the few oxide-based phases that exhibit substantial, permanent anion exchange capacity [Kirkpatrick, et al. 1999, Plamer, et al., 2009, and Zhang and Reardon, 2003]. They also contribute to the structural properties of cementitious matrices [Taylor, 1997].

The mineralogy of the cured cementitious material influences the physical properties (strength, stiffness, etc.) of the cured material due to the degree of polymerization (chain length) and tetrahedron arrangement. Information about the mineralogy of hydrated cementitious materials and blends of these ingredients is needed to design waste form matrices, select ingredients and make adjustments in material proportions. Information presented in this report is an initial step in developing phases diagrams for the hydrated systems in which caustic sodium salt solutions are used as the hydration fluid for waste forms.

ABBREVIATIONS

AAS	**Alkali Activated Slag**
ASTM	**American Society of Testing and Materials**
C-S-A-H	**Alumina Substituted Hydrated Calcium Silicate Gel (non to poorly crystalline solid)**
C-S-H	**Hydrated Calcium Silicate Gel (non to poorly crystalline solid)**
DOE	**US Department of Energy**
EDX	**Energy Dispersive X-Ray**
GGBFS	**Ground Granulated Blast Furnace Slag**
ICDD	**International Center for Diffraction Data**
LDH	**Layered Double Hydroxide**
M	**Molar**
MAS	**Magic Angle Scattering**
NMR	**Nuclear Magnetic Resonance**
ORNL	**Oak Ridge National Laboratory**
R&D	**Research and Development**
rpm	**Revolutions per minute**
SEM	**Scanning Electron Microscopy**
SRNL	**Savannah River National Laboratory**
TDS	**Total Dissolved Solids**
TT/QAP	**Task Technical and Quality Assurance Plan**

TABLE OF CONTENTS

LIST OF TABLES

INTRODUCTION

Cementitious materials are used to solidify and stabilize aqueous based radioactive waste containing sodium salts. The types and proportions of cementitious ingredients used to treat aqueous radioactive waste streams containing sodium salts depend on the performance objectives for the waste forms and the compositions of the waste streams. Matrix phases can stabilize certain contaminants (co-precipitation, substitution, ion exchange, and / or sorption), influence processing properties, and are responsible for physical properties and durability of the cured waste forms. Consequently, characterization of the matrix (binder) mineralogy (chemical compositions and crystalline / non crystalline structures) is important for predicting contaminant leaching and evolution of the materials as a function of time and changing conditions.

This report documents sample preparation and x-ray diffraction results for a series of mixtures of sodium salt waste and cementitious binders.

OBJECTIVE

The objective of this report was to characterize the phase assemblages in the Cementitious Barriers Partnership reference case sodium salt waste form [Langton, 2009]. This information can be used to: 1) generate a base line for the evolution of the waste form as a function of time and conditions, 2) potentially to design new binders based on mineralogy of the binder, 3) understand and predict anion and cation leaching behavior of contaminants of concern, and 4) predict performance of the waste forms for which phase solubility and thermodynamic data are available. Characterization of the mineralogy is also important for understanding the buffering effects that the waste form has on infiltrating water / leachates.

BACKGROUND

Sodium salt waste forms generated in the DOE complex typically consist of a blend of ground granulated blast furnace slag (GGBFS), portland cement, and Class F fly ash. Blends of these ingredients have been used to treat caustic aqueous sodium salt waste streams generated from separation and recovery of isotopes for defense programs. The objective of the treatment is to provide a diffusion barrier for soluble contaminants, stabilize selected contaminants, and convert a liquid waste into a solid waste form suitable for disposal.

This effort was intended to obtain preliminary phase / mineralogy data for subsequent electron and neutron diffraction analyses of the hydrated binder phases. An experimental plan to characterize the matrix phases was developed by SRNL researchers in conjunction E. Pierce, ORNL and documented in Task Technical and Quality Assurance Plan (TT/QAP) [Langton, 2012].

At the present time, the matrices of these cementitous waste forms are not well characterized because a large portion of the matrix is not well crystallized and because solid solutions and cation and anion substitutions in the calcium silicate hydrates (C-S-H) and magnesium aluminate hydrates and calcium aluminate hydrates can be extensive. In addition, the matrix consists of micrometer and submicrometer particles intergrown to the extent that individual particles are difficult to characterize using scanning electron microscopy (SEM) and energy dispersive x-ray spectroscopy (EDX).

EXPERIMENTAL METHOD

A simulated waste solution was prepared with water or a sodium salt solution based on the CBP reference case salt waste form. The simple salt solution composition is provided in Tables 1 and 2. This solution had a density of 1.207 g / ml and contained 25.13weight percent total dissolved solids (TDS).

Table 1. Sodium salt waste solution with a molar composition of a simple simulated sodium salt solution.

Component	M
Na	4.4E+00
Al	1.1E-01
Cr	5.8E-03
Re	1.6E-03
B	1.1E-02
K	5.4E-03
NO_3	2.2E+00
NO_2	3.7E-01
OH	1.8E+00
CO_3	1.4E-01
SO_4	4.6E-02
C_2O_4	9.3E-03
Cl	4.6E-03

Table 2. Ingredients used to prepare the simulated salt solution.

Compound	**g / L**
Water	balance
KNO_3	0.55
$NaNO_3$	154.37
NaOH (50%)	142.4
$Al(NO_3)_3 \cdot 9H_2O$	42.01
$NaNO_2$	25.66
Na_2CO_3	14.73
Na_2SO_4	6.59
Na_2CrO_4	0.94
$Na_3PO_4 \cdot 12H_2O$	1.9
$Na_2C_2O_4$	1.24
H_3BO_3	0.71
NaCl	0.27

The ingredients and proportions in the cementitious materials and mixtures prepared for x-ray diffraction characterization are provided in Table 3. Each mix was prepared as a large batch in a chemical fume hood using a paddle mixer with the blade set about 2 cm above the bottom of a 2000 ml beaker. The cementitious reagents were premixed by shaking them in a sealed plastic bag. The liquid was added to the beaker before the mixer was turned on and the rotational speed was adjusted to about 250 revolutions per minute (rpm). The corner of the bag containing the cementitious reagents was cut, and the contents of the bag were slowly added to the solution. After all of the solid reagents were added, the slurry was mixed for 3 minutes at a paddle speed adjusted to form a vortex but minimize air entrapment. After mixing, each mixture was cast into multiple 70 mL plastic containers. The containers were filled completely and capped. After setting on the bench top for 3 days the samples were over packed in a plastic bag to which a damp cloth was added to provide a moisture curing environment in case the caps were breeched. All samples were cured at ambient laboratory conditions.

Table 3. Material prepared for x-ray-diffraction characterization.

Sample No.	Sample Description (Ingredients and Proportions)					Water to cementitious materials mass ratio
	Portland cement I/II	Ground Granulated Blast Furnace Slag (Grade 100)	Class F fly ash	ASTM Type 1 water	.4 M Na Salt Waste Simulant	
	(g)					
448-1A, 1B, 1C	Anhydrous cement	--	--	--	--	NA
448-2A, 2B, 2C	--	Anhydrous slag	--	--	--	NA
448-3A, 3B, 3C	--	--	Anhydrous fly ash	--	--	NA
448-4A to 4G	500	--	--	300	--	0.60
448-5A to 5G	--	500	--	300	--	0.60
448-6A to 6G	--	--	500	300	--	0.60
448-7A to 7G	751	--	--	--	602	0.60
448-8A to 8G	--	751	--	--	602	0.60
448-9A to 9G	--	--	751	--	602	0.60
448-10A to 10G	150	601	--	--	602	0.60
448-11A to 11G	150	--	601	--	602	0.60
448-12A to 12G	--	375.5	601	--	602	0.60
448-13A to 13G	75	338	338	--	602	0.60

One sample of each material was sent to E. Pierce, Oak Ridge National Laboratory, Oak Ridge, TN, after curing for 28 days. The intent was to obtain x-ray diffraction powder patterns at the ORNL as a precursor to neutron diffraction analyses at the ORNL Spallation Neutron Source. The neutron diffraction analyses were to be arranged by E. Pierce.

In addition, D. M. Missimer, SRNL Analytical R&D Programs, performed x-ray diffraction analyses on identical samples cured for 14 months to evaluate the effect of curing time on the mineralogy. A Bruker DA Advance x-ray diffractometer with CuKα radiation (1.5405982 Å wave length) was used to generate the diffraction patterns. JADE x-ray analysis software from Materials Data Inc. was used to identify phases along with chemistry of the materials and information from the literature.

LITERATURE REVIEW

Portland cement, GGBFS and Class F-fly ash, and combinations of these materials have been extensively characterized in the literature. The review presented in this report is not intended to be in anyway comprehensive. Rather it is intended to illustrate that portland cement, GGBFS, Class F fly ash, and blends of these ingredients are multicomponent and multi-phase materials which have differing and variable compositions. In addition hydration products of these materials and blends are also multiphase. The mineralogy of the hydrated phases depends on many factors such as proportions of materials in blends, amount of water available for hydration, temperature, time, and other environmental conditions.

Portland cement: ASTM C-150 does not identify proportions of the phases in portland cement. Instead, oxide chemical requirements are identified and a method of estimating approximate phase proportions based on chemical analysis is provided. Phases and materials in Type I/II portland cement are listed in Table 4. Minor phases present in portland cement clinker may include: periclase (Mg) and sodium and potassium sulfate phases: arcanite, aphthitalite, and langbeinite.

Table 4. Portland cement mineralogy.

Phase	Cement Shorthand Terminology*
Cement clinker	
Ca_3SiO_5	C_3S Alite and polymorphs
Ca_2SiO_4	C_2S Belite, Larnite and polymorphs
$Ca_3A_2O_6$	C_3A
$Ca_2(Al_x,Fe_{1-x})_2O_5$ series	C_4AF where x = 0.5 Ferrite
K_2SO_4	$K_2\boldsymbol{S}$ Arcanite
$(K,Na)_3Na(SO_4)_2$	$(K,N)_3N\boldsymbol{S}_2$ Aphthitalite
$(K_2Mg_2(SO_4)_3$	$K_2M_2\boldsymbol{S}_3$ Langbeninite
MgO	M Periclase
Interground material	
Gypsum $CaSO_4{\cdot}_2H_2O$	$C\boldsymbol{S}$
Limestone (calcite $CaCO_3$ + mineral phases occurring in limestone)	$C\boldsymbol{C}$
Grinding aids and particle dispersants	Inorganic: fly ash or slag (< 3%) [Stutzman, 2014] Organic: e.g., aliphatic amines, complex amines, glycol compounds, phenol and phenolic derivatives [Katsioti, et al. 2009]

* The letters $\overline{C}$ and $\overline{S}$ overlain with a bar are used to represent SO_4^{2-} and CO_3^{2-} in conventional cement notation as are the bold italic letters ***C*** and ***S***.

Hydrated Portland Cement: Phases formed in Type I/II portland cement hydrated with a water to cement (w/c) ratio of 0.4 to 0.6 cured under ambient laboratory conditions are listed in Table 5. Hydration of portland cement results in calcium-rich gels with Ca/Si ratios between 1.5 and 2.0 Taylor, 1997]. These gels are often described as non-cross linked tobermorite and jennite-like structures [Myers, 2013].

Inner product C-S-H forms within the space originally occupied by either alite or belite grains in the portland cement and also in space originally occupied by slag grains. Outer product C-S-H forms in space originally filled by water. In hydrated portland cement paste the outer product typically contains a mixture of inter-grown portlandite and AFm and AFt phases and has a fibrous morphology. Slag loading alters this linear morphology from a fibrous to a foil-like morphology.

The inner product C-S-H typically displays a dense, coarse morphology. Rims of particles oriented perpendicular to the original grain boundaries are often formed around the alite, belite, and slag grains which may persist for years. The inner product can also contain laths or platelets of AFm and relicts of AFt needles [Richardson and Groves, 1992, and Taylor, 1997].

AFt phases have the general formula $[Ca_3(Al,Fe)(OH_6)]\cdot X_3\cdot xH_2O$, where X represents one formula unit of a doubly charged anion or 2 formula units of a singly charged anion.

AFm phases are layered double hydroxides (LDHs) and have a distorted layered structure derived from portlandite, $Ca(OH)_2$. The entire family of AFm phases is often grouped together as the hydrocalumite phases. In the simplest structures, one Ca^{2+} ion in three is typically replaced by Al^{3+} or Fe^{3+}. The Ca : Al ratio is 2:1 and SO_4^{2-}, CO_3^{2-}, or OH^- occupy the anion positions. The cation layers alternate with layers containing anions and H_2O. AFm phases typically found in hydrated portland cements and blended cements include: hydrocalumite or hydroxy AFm, $4CaO\cdot Al_2O_3\cdot 13\text{-}19\ H_2O$, hemicarboaluminate, $3CaO\cdot Al_2O_3\cdot[Ca[(OH)(CO_3)_{0.5}]\cdot xH_2O$, monocarboaluminate, $3CaO\cdot Al_2O_3\cdot CaCO_3\cdot xH_2O$, Friedel's salt, $3CaO\cdot Al_2O_3\cdot CaCl_2\cdot xH_2O$, and stratlingite, a calcium aluminate silicate hydrate. A large number of AFm minerals occur naturally and can sequester multivalent anions and cations.

Table 5. Hydrated Portland cement mineralogy (w/c = 0.4 to 0.6; ambient temperature curing).

Phase	Composition
C-S-H (inner product)	Ca/Si ~ 2
C-S-H (outer product)	Ca/Si ~ 1.5 to 1.1
Portlandite	Ca(OH)2
Ettringite (Aft)	$Ca_6Al_2(SO_4)_3(OH)_{12}\cdot 26H_2O$
Monosulfoaluminate (AFm)	$Ca_4Al_2(SO_4)(OH)_{12}\cdot 6H_2O$
Monocarboaluminate*	$Ca_4Al_2(CO_3)(OH)_{13}\cdot 5.5H_2O$
Hemicarboaluminate*	$Ca_4Al_2(CO_3)_{0.5}(OH)_{12}\cdot 5H_2O$
Hydrogarnet	$Ca_3[Al(OH)_6]_2$

* The presence of inter-ground fine limestone in the current portland cements is likely to produce carbonate hydrates.

Ground Granulated Blast Furnace Slag: GGBFS is produced by quenching molten iron slag in water or steam (wet quenching), then drying and grinding it into a fine powder. Dispersants are also used as grinding aids for size reducing slag. The main components of blast furnace slag are CaO (30-50%), SiO2 (28-38%), Al2O3 (8-24%), and MgO (1-18%). GGBFS is 90 to 100 % glass. The amount of glass depends on the cooling rate and temperature at which the quenching is initiated. GGBFS used in concretes and mortars is specified in ASTM C989. Crystallized slags contain minor amounts of reduced sulfur as CaS with varying amounts of Mg and Fe substituted for Ca. Li, et. al, 2011 concluded that GGBFS glass is separated into two phase: a Ca-rich phase and a Si-rich phase that approximates akermanite (Ca2Mg[Si2O7]). Most of the Si is distributed around Mg and calcium is associated with both Si and Al. Depending on the characterization techniques and slag preparation, micro- to nano-crystallites have been reported in GGBFS slag glasses.

Alkali Activated Slag (AAS): GGBFS is a glass and is slow to react with water. However, in the presence of alkali and water, it is activated and forms hydrated phases that are cementitious. For Na activated slag, the main hydration product is a sodium substituted calcium-aluminum-silicate hydrate, C(N)-A-S-H, typically with a lower Ca/Si ratio (1.1 to 1.2, i.e. close to the ratio in unreacted slag) and higher Al/Si ratio than the C-S(A)-H resulting from ordinary portland cement hydration [Richardson and Groves, 1992]. The aluminum substituted gel is charge balanced with alkali and the gel structure can be described as tobermorite-like with the possibility of some cross-linking between the tobermorite chains [Myers, et.al, 2013]. The C-S-H gel formed in hydrated cement-slag mixtures is reported to be more like that formed from portland cement hydration (no cross-linking) and forms along with calcium hydroxide [Taylor, 1997].

Poorly crystalline layered double hydroxide (LDH) hydrotalcite-like phase, $Mg_6Al_2(OH)_{16}CO_3 \cdot 4H_2O$, is characteristic of GGBFS hydration. Hydrotalcite is structurally related to brucite in a way that is analogous to AFm phases being related to portlandite. Some of the Mg ions may be replaced by Al^{3+} and Fe^{3+} and the charge is then balanced by anions which together with H_2O molecules occupy interlayer sites with accompanying anion exchange [Taylor, 1998]. The layer thicknesses are similar to AFm phases it is difficult to distinguish between the two groups of phases by x-ray diffraction if only the basal reflections are observed.

Other phases formed from alkali activated slag include: Fe-rich cubic hydrogarnet, $Ca_3[Al(OH)_6]_2$ and one or more AFm phases, $Ca_2(Al,Fe)(OH)_6]\cdot X\cdot xH_2O$ where X is one formula unit of a singularly charged anion or half of a formula unit of a doubly charged anion. Examples of phases depend on the oxide composition of the slag and include: $C_4AH_{13,}$tetracalcium aluminum hydrate; $C_2ASH_{8,}$ stratlingite, $Ca_2Al_2(SiO_2)(OH)_{10}\bullet 2.5(H_2O)$; and/or $C_4AH_{12,}$ hydrocalumite, $Ca_4Al_2(OH)_{12}(CO_3,OH)_2\cdot 4H_2O$ [Chen and Brouwers, 2007 and Taylor, 1997].

The type of alkali used to activate the slag has an effect on the reaction products. NaOH activation of GGBFS results in poorly-ordered C-S-H with a foil like morphology and Ca/Si = 0.9 to 1.0 (lower than in the starting slag) and Na/Al of 2.0 to 2.22. This gel has a dreierkette-type structure (three chain structure). The relatively long linear chains correlate with mechanical strength. The mean chain length is about 8 tetrahedra [Fernandez-Jimenez and Puertas, 2003, Schilling et. al, 1994 and Richardson et. al 1982]. Other phases found in NaOH activated slag included: calcite, hydrotalcite, and carboaluminates.

Based on ^{29}Si and ^{27}Al magic-angle spinning (MAS) nuclear magnetic resonance (NMR) spectroscopy, Na_2CO_3 activated slag also results in poorly-ordered C-S-H with a foil like morphology with a lower Ca/Si ratio than that formed from NaOH activation. The strengths of the Na_2CO_3 activated slag gels are higher than those formed from NaOH activated slag. The highest strengths were obtained from sodium silicate (water glass) activation which resulted C-S-H formed from highly condensed anions which favored formation of cross-linked structures that contributed to increased mechanical strength [Fernandez-Jimenez and Puertas, 2003].

Class F Fly Ash: Class F fly ash is a byproduct of burning bituminous coal in a coal-fired electric and steam producing power plants. The fly ash material solidifies while suspended in the exhaust gases and is collected by electrostatic precipitators or filter bags before the gases are discharged. Since the particles solidify rapidly, fly ash particles are generally cenospheres, (single spheres, joined spheres, or spheres with in spheres), and range in size from < 0.5 µm to 300 µm. Due to the rapid cooling, most of the fly ash is amorphous (glass). Crystalline phases in fly ash are refractory phases in the coal or that form from minerals in the coal. These crystalline phases are typically coated with and incorporated in the glass cenospheres and plerospheres (hollow spheres filled with smaller spheres) and can be revealed through selective dissolution or microscopy. In summary, fly ash is a heterogeneous material. The main phases encountered are a glass phase, together with quartz, mullite, and the iron oxides hematite, magnetite and/or maghemite. Other phases often identified are cristobalite, anhydrite, free lime, periclase, calcite, rutile and anatase. Examples of fly ash mineralogy are provided in Table 6. Detailed structural analysis of the amorphous material in Class F fly ash suggests that the glass is not homogeneous at the time it is quenched [Bumrongjaroen, et.al, 2007].

Hydrated Class F Fly Ash: Class F fly ash is mostly inert when exposed to water and air. However, when calcite, $CaCO_3$, is detected in Class F fly ash it is an indication that the ash contained a small amount of CaO which typically hydrates and then carbonates. Class F fly ash is pozzolanic and reacts with calcium and water to produce a cementitious material. Geopolymers can also be formed from Class F fly ash when activated by alkali solutions such as sodium hydroxide or sodium silicate (water glass).

Table 6. Hydrated Slag Mineralogy.

	Taylor, H.F.W., Cement Chemistry, 2nd ed., 1997		**Fernandez-Jimenez, A. and F. Puertas, J. Am Ceram. Soc. 86(8) 1389-94 (2003)**		
Phase	**Cement Activated Slag (1:1)**	**Alkali Activated Slag (3.5-5.5M NaOH)**	**NaOH Activated Slag**	**$NaCO_3$ Activated Slag**	**Na Silicate Activated Slag (water glass)**
C-S-H	Ca/Si ~1.55 Al/Ca ~ 0.09	C-S-H(I) relatively highly ordered Ca/Si ~1.1 to 1.2 Al/Ca ~0.19 Al in C-S-H substituted exclusively in bridging sites of dreierketten w/mean chain length 4.83 tetrahedron	C-S-H with dreierkette-type (3 chain) structure shows high Q2 Si values indicative of long linear chains but no Q3 Si values, i.e., low strength. Semi-crystalline, Foil like morphology Ca/Si = 0.9-1.0 (lower than starting slag) Na/Al = 2.0-2.22 Tetrahedral condensation ratios are higher in NaOH AAS and Water glass activated than in Na_2CO_3 AAS indication Al is incorporated in tet chains with charge balanced by Na+ (TEM/EDS).	C-S-H shows low Q3 Si values. Med. Strength Semi-crystalline, Foil like morphology Ca/Si = 0.9 to 1.0 (lower than in the starting slag)	C-S-H with highly condensed anions, Si in Q2 and Q3 sites which favors formation of cross-linked structures that result in increased strength
$CaCO_3$	Not mentioned	Not mentioned	Yes	Yes	--
Hydrotalcite-type phase $Mg_6Al_2(CO_3)(OH)_6 \cdot 4(H_2O)$	Mg/Al = 3 to 2.5 if Fe replaces Al	--	Yes	Yes	--
AFm phase	--	possible	--	--	--
AFm Carboaluminate phase(s) of the C4A*C*3H11-Type	--	--	Yes	Yes	--
Zeolites	Formed at temp. > 120 ºC in hydrated systems	Formed at temp. > 120 ºC in hydrated systems	Zeolite formation requires high Al/Si and low Ca/Si	Not mentioned	--
$Na_2Ca(CO_3)_2 \cdot 0.5\ H_2O$	--	--	--	Yes	--

Table 7. Class F fly ash mineralogy.

Phase	**Taylor, H. F. W. Cement Chemistry, 2nd ed. , 1997**	**Bumrongjaroen, W., I. S. Muller, and I. L. Pegg, 2007 VSL-07R520X-1**	**McCarthy, G. J., 1988**
Glass	Cu Kα peaks around 22-23° 2θ	71.9 wt. % Mullite-rich ~ 53.6 Class F glass ~ 24.1 Spinel rich ~ 12.8 Low-silica glass ~ 5.8 Class C glass ~ 2.0 Quartz rich ~ 1.7	x
Mullite **$Al_6Si_2O_{13}$** **prisms in glass**	x	18.9	x
Quartz **SiO_2** **prisms in glass or angular particles**	x	6.7	x
K_2SO_4 **particles adhering to spheres**	x	--	--
$CaSO_4$ **particles adhering to spheres**		Trace	--
Hematite **Fe_2O_3** **particles adhering to spheres or separate particles**	x	1.07	x
Magnetite **Fe_3O_4** **particles adhering to spheres or separate particles**	x	1.13	x
Ferrite Spinel **Sub Mg, Al, Ti, Ni, Cr**	--	0	Al substituted for Fe and could be misidentified as magnetite [Wingurn, R. S., S.S. Lerach, G. J. McCarthy, 2000 JCPDS Data Advances in X-ray Analysis V. 43, p.350]
Carbon **Porous particles**	x	Not determined	Not determined
Cenospheres (hollow)		Not evaluated	Not evaluated
Plerospheres (spheres filled with other spheres or particles)		Not evaluated	Not evaluated

RESULTS

X-ray powder diffraction is one of several complimentary techniques for identifying phases in solid materials. In this study, an attempt was made to identify changes in the mineralogy starting with the anhydrous cement, slag, and fly ash and progressing to characterization of these materials hydrated with water and also with sodium salt solution. Characterization of the reaction products of selected blends of these cementitious reagents resulting from hydration in water and salt solution was also performed.

Anhydrous starting materials: Phases present in the anhydrous Type II portland cement, Grade 100 GGBFS, and carbon burn-out (CBO) Class F fly[1] ash are listed in Table 7. The mineralogy of these materials is consistent with the phases reported in the literature. The x-ray diffraction techniques used in this study can detect minor amounts (below about 3 weight percent) of crystalline phases in the samples. Broad very low intensity peaks are indicative of anhydrous and hydrated poorly ordered silicate based phases in the powder x-ray diffraction patterns.

The portland cement, Sample 1A, contained alite (Ca_3SiO_5), larnite (Ca_2SiO_4), a ferrite phase ($Ca_2(Al,Fe)O_5$) and calcite ($CaCO_3$). Neither gypsum nor anhydrite was detected in the x-ray patterns although it is known to be inter-ground with the cement to control initial hydration reactions. Since this cement contains tricalcium aluminate ($Ca_3A_2O_6$) below the detection limit for x-ray diffraction, the amount of calcium sulfate required to control hydration of this phase is probably also low.

The Grade 100 slag, Sample 2A, is predominantly a silicate glass (non-crystalline material) containing a trace amount of akermanite ($Ca_2Mg[Si_2O_7]$), a refractory calcium magnesium silicate phase that formed during the slag production. Calcite was also detected in the x-ray diffraction pattern.

The Class F fly ash, Sample 3A, is also a glass (non-crystalline) which contains mullite ($Al_6Si_2O_{13}$) and quartz (SiO_2). The mullite formed as a refractory aluminum silicate phase when clays in the coal were melted and were subsequently crystallized. The quartz is a residual phase from the coal itself.

Hydration of starting materials in water: Phases detected in the cementitious starting materials hydrated in water are also listed in Table 7. These samples were cured in sealed containers at room temperature for 2 and 14 months. The amount of non-crystalline or poorly crystalline C-S-H in the cement + water samples, 4A and 4G, increased between 2 and 14 months. Ettringite, an AFt phase, $Ca_6Al_2(SO_4)_3(OH)_{12}\cdot 26H_2O$, calcium aluminum sulfate hydrate, and a trace amount of an AFm phase, probably monosulfoaluminate were detected in the x-ray patterns.

Unreacted anhydrous glass material was the predominant phase in the GGBFS samples 5A and 5G cured for 2 and 14 months, respectively. However, hydration of the slag in water resulted in formation of a small amount of a hydrotalcite-type phase[2] or a mixture of hydrotalcite and hydrocalumite (AFm), which was observed in pattern for the 14 month old sample (Samples 5G). C-S-H may be present in the sample but SEM/EDX or other techniques are required to determine whether it formed. Calcite and possibly akermanite, present in the unreacted slag, were also detected in the GGBFS hydrated in water for 2 and 14 months.

---

[1] Carbon Burn Out consists of combusting residual carbon in fly ash to produce a consistent, low carbon (< 2.5 wt. %) high quality pozzolan. The drivers for CBO are to control the amount of carbon in fly ash to levels acceptable for construction applications and to eliminate ammonia contamination of the ash. Introduction of low NOx burners in recent years at coal fired power plants has resulted in increased levels of residual carbon in the ash. Also ammonia injection is used in some plants to enhance electrostatic precipitator performance and is being applied in selective catalytic reduction and selective non-catalytic flue gas treatment systems to meet the new more stringent NOx off gas standards. (Removal of ammonia is considered for fly ash containing more than about 50 -100 ppm if it is to be used in concrete applications.)

[2] Hydrotalcite-type phases are layered double hydroxides (LDHs) with metal cations in the main layers and anion and water in the interlayers. They are structurally related to brucite, $Mg(OH)_2$. The general formula is $Mg_6Al_2(OH)_{16}$.

Table 8. Phases identified in XRD powder patterns of anhydrous cementitious reagents and individual hydrated materials and the corresponding International Center for Diffraction Data (ICDD) database card numbers.

Material	Sample No. (Cure Time)	Glass NCS	Hydrated NCS	CSH 034-0002	11Å Al-Tobermorite 019-0052	Hydrotalcite 041-1428	Hydrocalumite AFm 031-0245	Ettringite AFt 041-1451	Portlandite 004-0733	Ca_3SiO_5 049-0442	Ca_2SiO_4 033-0902, 033-0302	Brownmillerite $Ca_2(Al,Fe)O_5$ 042-1469	Gypsum 033-0311	Quartz SiO_2 046-1045	Mullite $Al_6Si_2O_{13}$ 015-0776	Akermanite 035-0592	Calcite $CaCO_3$ 005-0586	Natratine $NaNO_3$ 036-1474	Comments
Type II cement	1A	--	--	--	--	--	--	--	--	X	X	X	--	--	--	--	x	--	
Grade 100 slag	2A	X	--	--	--	--	--	--	--	--	--	--	--	--	--	?	?	--	
Class F Fly ash	3A	X	--	--	--	--	--	--	--	--	--	--	--	X	X	--	--	--	
Type II Cement + Water	4A (2 mo.)	--	?	?	?	x	--	X	X	--	?	--	--	--	--	--	--	--	Bad pattern
	4G (14 mo.)	--	X	--	?	x	--	X	X	X	--	--	?	--	--	--	--	--	? Calcium iron sulfate hydrate 040-0292
Slag + Water	5A (2 mo.)	X	?	?	?	--	--	--	--	--	--	--	--	--	--	--	--	--	
	5G (14 mo.)	X	?	--	--	x	?	--	--	--	--	--	--	--	--	x	x	--	
Fly ash + Water	6A (2 mo.)	X	--	--	--	--	--	--	--	--	--	--	--	X	X	--	--	--	
	6 (14 mo.)	Not evaluated																	

X = Several major peaks identified. x = Peaks identified with low relative intensity. ? = Peaks overlap other peaks, no unique peak identified, Tr = Identified based on small peaks and chemistry. -- = Not identified.

Table 9. Phases identified in XRD powder patterns of individual cementitious materials hydrated with 5 M Na salt solution and the International Center for Diffraction Data (ICDD) Database Card Numbers.

Material	Sample No. Cure Time (mo)	Silicate Glass NCS	C-S-H Hydrated NCS	CSH I 034-0002	11Å Al-Tobermorite 019-0052	Hydrotalcite 041-1428	Hydrocalumite 031-0342	Ettringite 041-1451	Hydrogarnet	Portlandite 004-0733	Ca_3SiO_5 049-0442	Ca_2SiO_4 033-0902	$Ca_2(Al,Fe)O_5$ 042-1469	Gypsum 033-0311	Quartz 046-1045	Mullite 015-0776	Akermanite 035-0592	Calcite 005-0586	$NaNO_3$ 036-1474	Comments
Cement + Salt Solution	7A (2)	--	X	--	--	--	x 049-0457	--	--	X	--	x	--	--	--	--	--	--	X	
	7E (14)	--	X	--	--	--	x 049-0457	--	--	X	--	x	--	--	--	--	--	--	X	
Slag + Salt Solution	8A (2 mo.)	?	X	X	X	X	?	--	--	--	--	--	--	--	X	--	--	--	X	
	8B (14 mo.)	?	X	X	X	X	?	--	--	--	--	--	--	--	X	--	--	--	X	
Fly ash + Salt Solution	9A (2 mo.)	X	--	--	--	--	--	--	--	--	--	--	--	--	X	X	--	--	X	Low Counts
	9F (14 mo.)	X	--	--	--	--	--	--	--	--	--	--	--	--	X	X	--	--	X	X

X = Several major peaks identified. x = Peaks identified with low relative intensity. ? = Peaks overlap other peaks, no unique peak identified, Tr = Identified based on small peaks and chemistry, -- = Not identified.

Class F Fly ash was essentially inert in the presence of water (samples 6A). The same phases present in the unhydrated the CBO Class F fly ash were detected in the material exposed to water for 2 and 14 months, i.e. glass, and the refractory phases mullite and quartz.

Hydration of Starting Materials in 5 M Na Salt Solution: Phases detected in samples of the starting reagents, Type I/II portland cement, GGBFS, and CBO Class F fly ash, hydrated in 5 M Na salt solution are listed in Table 9. The phases detected by x-ray diffraction for the cement hydrated in salt solution samples (7A and 7E) included: C-S-H amorphous phase, portlandite, an AFm phase (calcium aluminate sulfate hydrate), unreacted larnite, and nitratine ($NaNO_3$) a component in the salt solution / pore solution.

Based on the powder pattern phase identifications, hydration of GGBFS in 5 M Na solution (Samples 8A and 8G) resulted in formation of fairly well crystallized material containing C-S-H I and aluminum substituted 11 Å tobermorite, in addition to a hydrotalcite-like phase and / or a mixture of hydrotalcite- and hydrocalumite-like phases. Some amorphous material, either unreacted glass or C-S-H, may also be present in samples cured for 2 and 14 months. Other characterization techniques are required to determine if residual slag or C-S-H or other amorphous phases are present. Quartz and a calcium iron oxide were identified based on d-spacings but were not detected in the slag and could not have formed during hydration. Addition work is being performed to obtain reasonable phase identification for those d-spacings.

No additional crystalline phases were detected in the Class F fly ash cured in 5 M Na salt solution (Samples 9A and 9F). Residual mullite and quartz were detected in the x-ray diffraction patterns along with amorphous material. The amorphous is probably a mixture of glass and hydrated glass. Exposure to caustic solutions results in partial to complete dissolution of the fly ash cenospheres.

Hydration of Blends in Salt Solution: Samples 10 A and B were prepared with a 1 : 3 mixture by weight of cement : slag that was hydrated with 5 M Na salt solution. They were hydrated for 2 and 14 months, respectively. Both samples contained fairly well ordered C-S-H II and aluminum substituted 11 Å tobermorite in addition to more than one AFm-type phase, either hydrotalcite or a mixture of hydrotalcite and hydrocalumite. Amorphous C-S-H or residual slag glass may also be present but other techniques are for complete characterization. Larnite (from the anhydrous cement) and akermanite and calcite (from the anhydrous slag) were also detected in trace amounts. $NaNO_3$ was also present in the x-ray diffraction patterns. Unreacted slag glass may be present but could not be differentiated from the amorphous C-S-H phase. The samples cured for 2 and 14 months had similar phase assemblages.

Samples 11 A and 11G were prepared with a 1 : 3 mixture of cement : Class F fly ash which was hydrated for 2 and 14 months with 5 M Na salt solution. The reaction product in these samples was primarily non-crystalline C-S-H. Residual larnite, mullite, and quartz were also detected in both samples in addition to $NaNO_3$. The 2 and 14 month old samples do indicate changes in the AFm calcium aluminate (sulfate) hydrate phases as a function of curing time. More detailed characterization is required to determine the composition and structure of these layered hydrates.

Samples 12 A and 12F were prepared with an approximately 2 : 3 mixture of slag and fly ash and cured for 2 and 14 months, respectively. These samples contained non-crystalline C-S-H and one or more layered double hydroxide phases (hydrotalcite, hydrocalumite, carboaluminate phase or a mixture of these phases) in addition to residual mullite, quartz, and $NaNO_3$. Crystalline C-S-H I and Al substituted tobermorite were not formed in this blend.

Samples 13 A and 13G Were prepared with a 10 : 45 : 45 mixture of cement : slag : fly ash and cured for 2 and 14 months, respectively. These samples contained mainly non-crystalline C-S-H and hydrotalcite. Trace amounts of CSH I and / or Na substituted 11 Å tobermorite (2-theta of 6-7º) and one or more

Table 10. Phases identified in XRD powder patterns of blends of cementitious materials hydrated with 5 M Na salt solution and the International Center for Diffraction Data (ICDD) Database Card Numbers.

Material	Sample No. Cure Time (mo)	Glass NCS	Hydrated NCS	CSH I 034-0002	11Å Al-Tobermorite 019-0052	Hydrotalcite 041-1428	Hydrocalumite 031-0245	Ettringite 041-1451	Hydrogarnet	Portlandite 004-0733	Ca_3SiO_5 049-0442	Ca_2SiO_4 033-0902, 033-0302	$Ca_2(Al, Fe)O_5$ 042-1469	Gypsum	Quartz 046-1045	Mullite 015-0776	Akermanite 035-0592	Calcite 005-0586	$NaNO_3$ 036-1474	Comments
Cement + Slag + Salt Solution	10A (2 mo.)	?	X?	X	X	X	?	--	--	--	x	x	--	--	--	--	x	x	X	061-0217 $CaAl_2O_410{\cdot}H_2O$
	10B (14 mo.)	?	X?	X	X	X	?	--	--	--	--	x	--	--	--	--	x	x?	X	061-0217 $CaAl_2O_410{\cdot}H_2O$
Cement + Fly Ash + Salt Solution	11A (2 mo.)	?	X	--	--	--	x	--	--	--	--	x	--	--	X	X	--	--	X	
	11C (14 mo.)	?	X	--	--	--	--	?	--	--	--	x	--	--	X	X	--	--	X	Possibly 2 new phases K_2SO_4, $NaAl(AlSi_3)O_{10}(OH)_2$
Slag + Fly Ash + Salt Solution	12A (2 mo.)	?	X	--	--	--	X	--	--	--	--	--	--	--	X	X	--	--	X	
	12F (14 mo.)	?	X	--	--	--	X	--	--	--	--	--	--	--	X	X	--	--	X	
Cement + Slag + Fly Ash + Salt Solution	13A (2 mo.)	?	X	--	--	X	??	--	--	--	--	--	--	--	x	x	?	?	X	
	13G (14 mo.)	?	X	?	--	X	??	--	--	--	--	--	--	--	X	X	?	x	X	

X = Several major peaks identified. x = Peaks identified with low relative intensity. ? = Peaks overlap other peaks, no unique peak identified, Tr = Identified based on small peaks and chemistry, -- = Not identified.

layered double hydroxide phases (hydrotalcite, hydrocalumite, or a mixture of these phases) in addition to residual mullite, quartz, calcite, and possibly akermanite in addition to NaNO3. The amount and /or the degree of crystallinity of the C-S-H I or tobermorite phase may be slightly higher in the sample cured for 14 months.

CONCLUSIONS

The mineralogy of the reaction products for materials and blends of materials hydrated with caustic 5 M Na salt solution depended on the mineralogy and proportions of the cementitious ingredients and the bulk oxide compositions of the mixtures. Poorly ordered /amorphous C-S-H was detected in mixtures of cement and slag, cement and fly ash, slag and fly ash and the waste form blend containing cement, slag, and fly ash when hydrated with caustic 5 M Na salt solution. Only the neat slag and cement + slag mixture hydrated with caustic 5 M Na salt solution contained fairly well crystallized C-S-H I and Al substituted 11 Å tobermorite.

Hydrotalcite and hydrocalumite-like phases and mixtures of these LDH phases were present in the all of the blended samples. However the proportions of these phases and probably their compositions varied. Not surprisingly, the phase assemblage in the 10:45:45 blend of cement : slag : fly ash resembled that of the slag : fly ash blend.

The mineralogy of the hydrated materials evaluated did not change significantly between 2 months and 14 months curing in sealed containers. Characterization of samples cured for much longer times is recommended. Both drying conditions and curing in the presence of excess water are may (are expecte to) result in changes in the mineralogy.

Cement hydrated for up to 14 months in water and up to 14 months in salt solution contained, poorly crystalline to non-crystalline C-S-H, portlandite ($Ca(OH)_2$), and an AFm phase. The AFm phase identified in the salt solution hydrated sample was a sodium aluminate sulfate. Ettringite, an Aft phase ($Ca_6(Al,Fe)_2(OH)_{12}(SO_4)_3.26H_2O$) was identified in the water hydrated cement sample but not in the salt solution hydrated sample. Unreacted larnite (Ca_2SiO_4) from the cement and $NaNO_3$ from the salt solution were detected in the salt solution hydrated sample.

Class F fly ash showed no significant reaction with water in the samples hydrated for 2 and 14 months. Hydration of the fly ash in salt solution resulted in dissolution of some of the glassy material as indicated by residual mullite “baskets”. The only crystalline phases detected in the x-ray diffraction patterns were the refractory phases, mullite and quartz, present in the anhydrous fly ash.

GGBFS did not hydrate or hydration was very limited after 2 months in water based on x-ray diffraction results. However, after 14 months, a small amount of LDH phase (hydrotalcite and / or hydrocalumite (AFm) or a mixture) was detected in the x-ray pattern. In contrast, activation of the slag in the 5 M Na salt solution resulted in formation of fairly well crystallized C-S-H I and Al substituted 11 Å tobermorite ($Ca_5Si_3Al(OH)O_{17}\cdot5H_2O$). These two ordered calcium silicate hydrates were detected in slag and mixtures of slag and cement hydrated with 5 M Na salt solution.

The mineralogy of the cured cementitious material influences the physical properties (strength, stiffness, etc.) of the cured material due to the degree of polymerization (chain length) and tetrahedron arrangement. Information about the mineralogy of hydrated cementitious materials and blends of these ingredients is needed to design waste form matrices, select ingredients and make adjustments in material proportions. Information presented in this report is an initial step in developing phases diagrams for the hydrated systems in which caustic sodium salt solutions are used as the hydration fluid for waste forms.

REFERENCES

Bumrongjaroen, W., I. S. Muller, and I. L. Pegg, 2007. "Characterization of Glassy Phase in Fly Ash from Iowa State University", VSL-07R520X-1, Vitreous State laboratory, Washington DC, 2007.

Chen, W, H. J. H. Brouwers, 2007. "The hydration of slag, Part 1: Reaction models for alkali-activated slag," J. Mater. Sci. 42:428-443.

Chen, W, H. J. H. Brouwers, and Z. H. Shui, 2007. "Three-dimensional computer modeling of slag cement hydration," J. Mater. Sci., 42:9595-9610.

Katsioti, M, P.E. Tsakiridis, P. Giannatos, Z.Tsibouki, and J. Marinos, 2009. "Characterization of various cement grinding aids and their impact on grindability and cement performance," Construction and Building Mat., 23(5):1954-1959.

Keppeler, J.G. and W.T.Frady, 2009. "Carbon Burn-Out, commercialization and experience update," http:/www.pmiash.com/cbo/acaa01paper.html.

Kirkpatrick, R. J., P. Yu, X Hou, and Y. Kim, 1999. "Interlayer structure, anion dynamics, and phase transitions in mixed-metal layered hydroxides: Variable temperature 35Cl NMR spectroscopy of hydrotalcite and Ca-Aluminate hydrate (hydrocalumite)," Am. Min. 4:1186-1190.

Langton, C.A. and H.H. Burns, 2012. "Characterization of phases in Savannah River Site saltstone using neutron diffraction at the ORNL Spallation Neutron Source, Task Technical and Quality Assurance Plan (TT/QAP)", SRNL-RP-2012-00448, Savannah River National Laboratory, Aiken, SC 29801.

Langton, C.A., D.S. Kosson, A.C. Garrabrants, and K.G. Brown, 2009. "Reference cases for us in the Cementitious Barriers Partnership Project," SRNL-STI-2009-00005, WM Symp, 2009.

Li, Chao, H. Sun, and L.Li, 2011. "Glass phase structure of blast furnace slag," *Advanced Materials Research*, 168-170:3-7.

Matschei, T., B. Lothenbach, F.P. Glasser, 2007. The AFm phase in portland cement," Cem. And Concrete Res. 37:118-130

McCarthyG. J., 1988. "X-ray powder diffraction for studying the mineralogy of fly ash." Fly ash and coal conversion by-products: characterization, utilization and disposal," Mat. Res. Soc. Proc., 113:75-86.

Myers, R. J., S. A. Bernal, R.S.Nicolas, and J. L. Provis, 2013. "Generalized structural description of calcium-sodium aluminosilicate hydrate gels: The cross-linked substituted tobermorite model," Langmuir, 29:5294-45406.

Palmer, S.J., T. Nguyen, and R. L. Frost, 2009. "Hydrotalcites and their role in coordinatin of anioinsin Bayer liquors: Anion binding in layered double hydroxides," Coordination Chemistry Reviews 253(1-2):250-267.

Richardson, I.G. and G. W. Groves, 1992. "Microstructure and microanalysis of hardened cement pastes involving ground granulated blast-furnace slag," J. Mater. Sci. 27:6204-6212.

Stutzman, P., 2014. Personal communication.

Taylor, H. F. W, 1997. Cement Chemistry, 2nd ed., Thomas Telford, NY, NY.

Zhang, M and E. J. Reardon, 2003. "Removal of B, Cr, Mo, and Se from wastewater by incorporation into hydrocalumite and ettringite," Environ. Sci. Technol., 37(13):2947-295.

Attachment 1. X-Ray Diffraction Powder Patterns

Materials Data Inc., JADE 20/10 software was used to analyze the diffraction patterns. Due to the complex patterns and presence of poorly crystalline and amorphous material in a few cases the software identified refractory phases which could not be present.

Anhydrous Cementitious materials

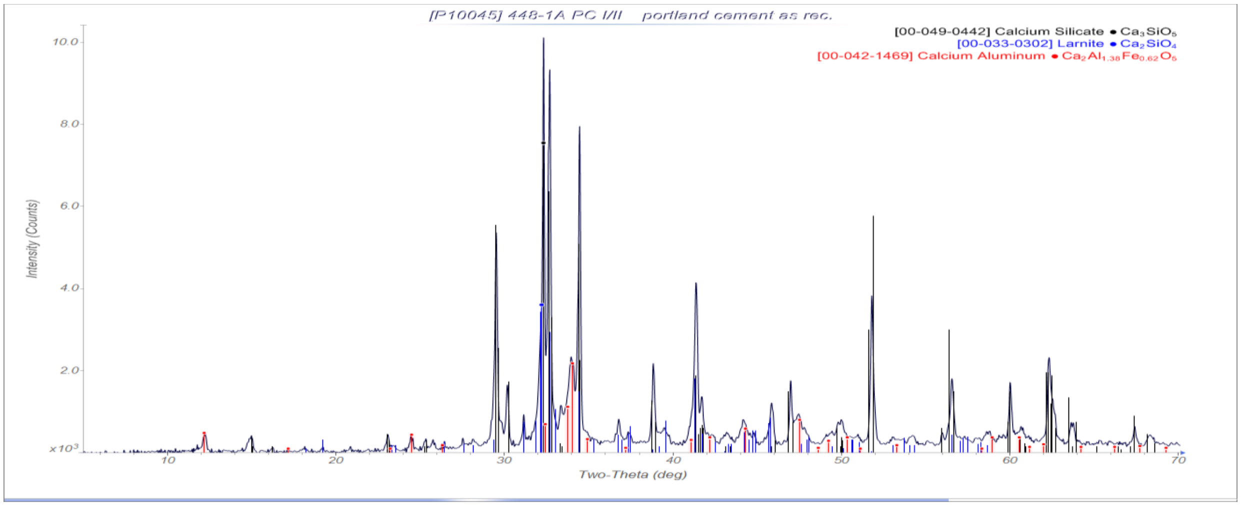

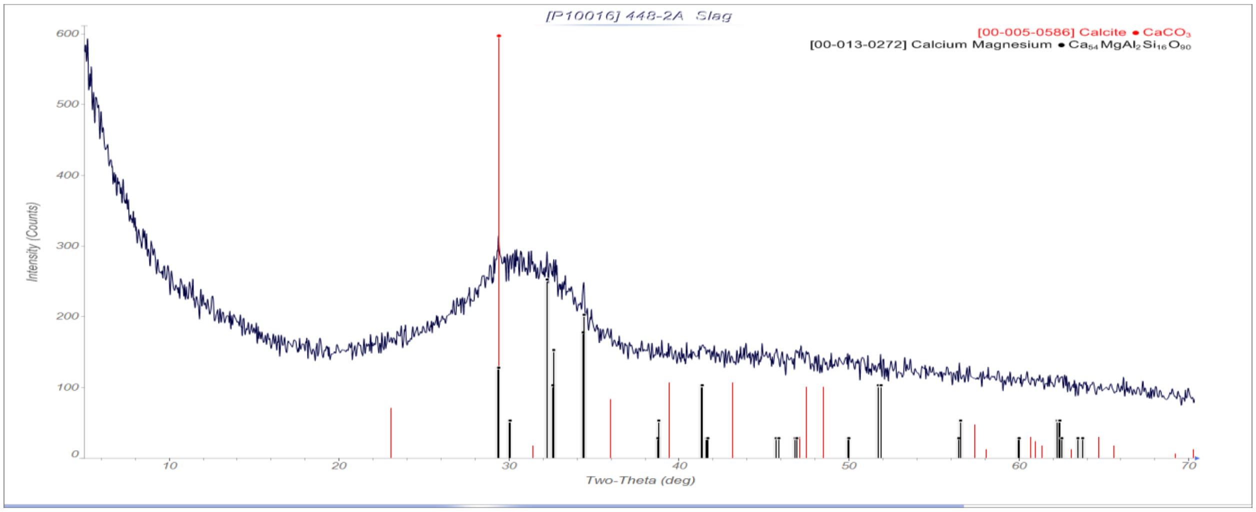

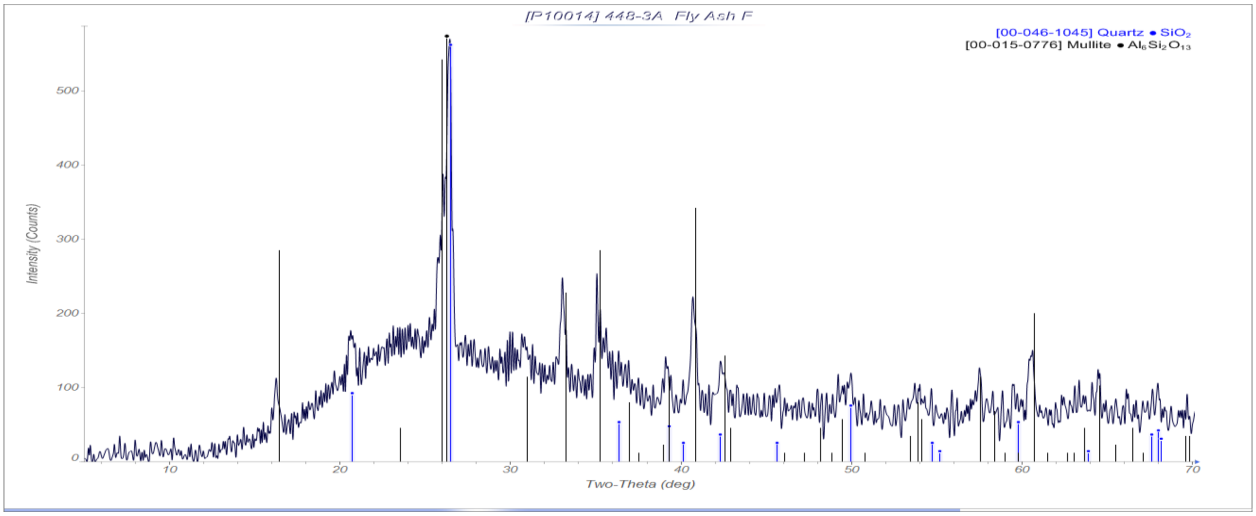

Water Hydrated Cementitious Reagents

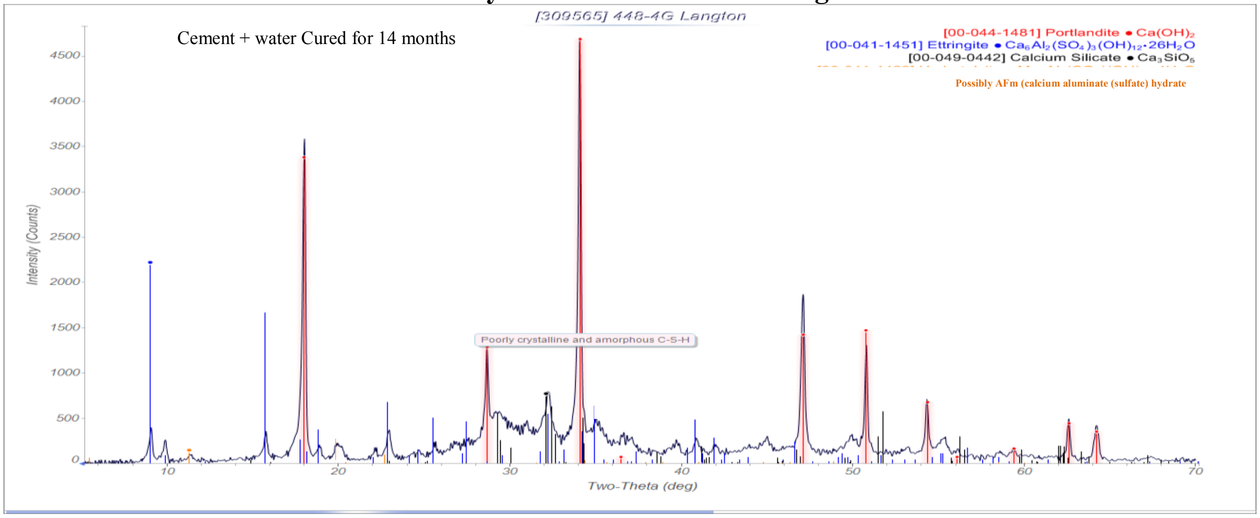
Cement + water Cured for 14 months

Possibly AFm (calcium aluminate (sulfate) hydrate

Poorly crystalline and amorphous C-S-H

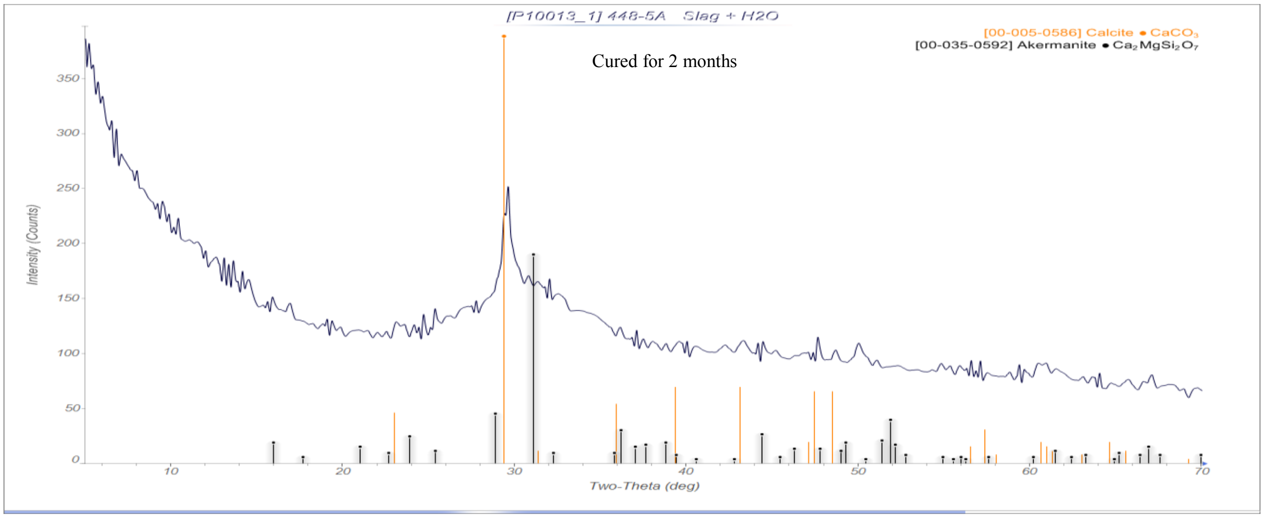
Cured for 2 months

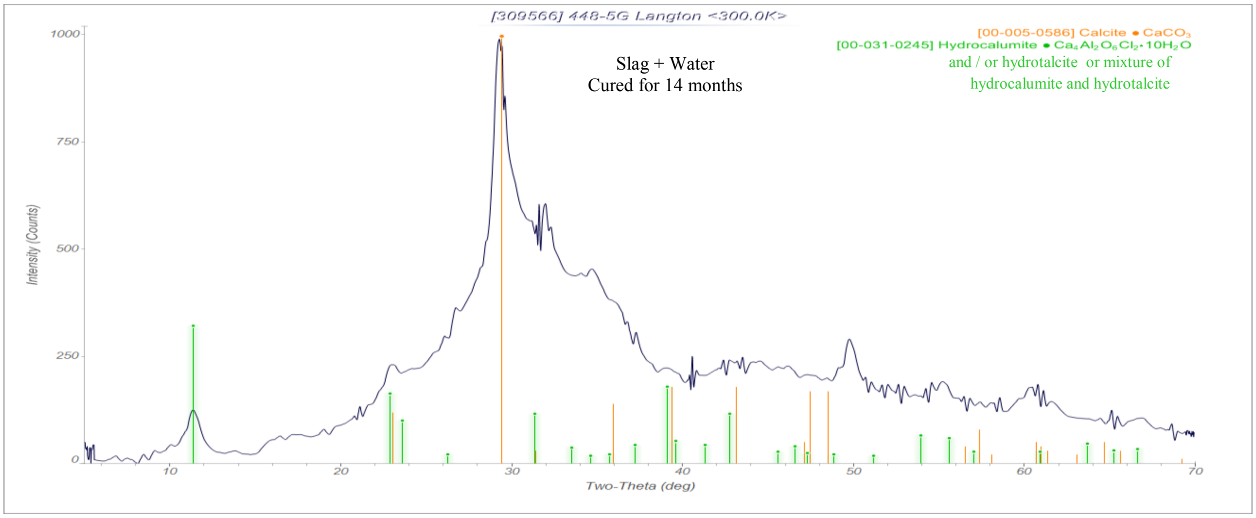
Slag + Water
Cured for 14 months

and / or hydrotalcite or mixture of hydrocalumite and hydrotalcite

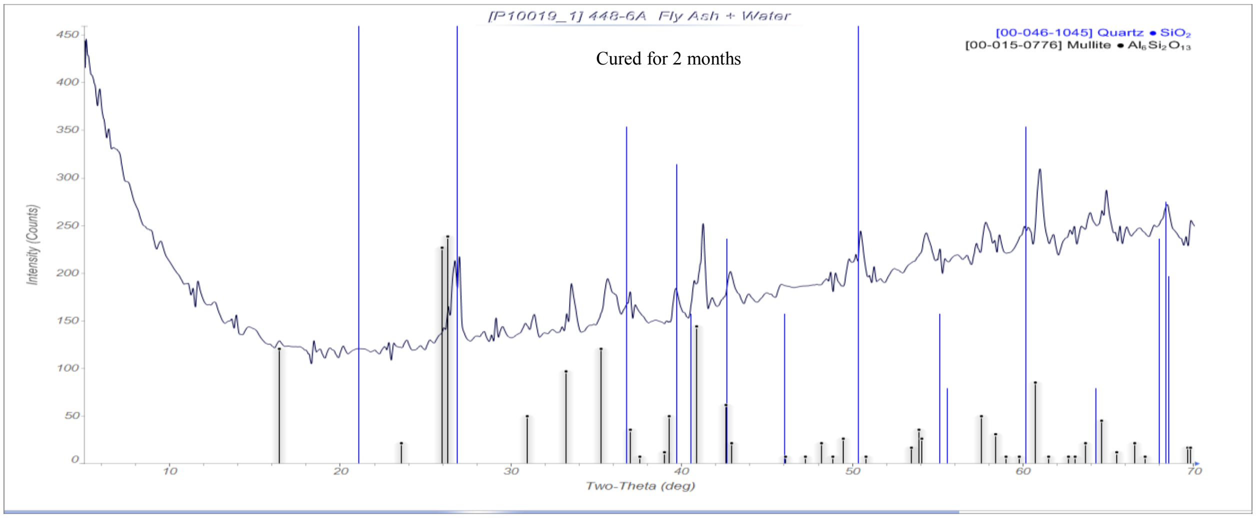

Cured for 2 months

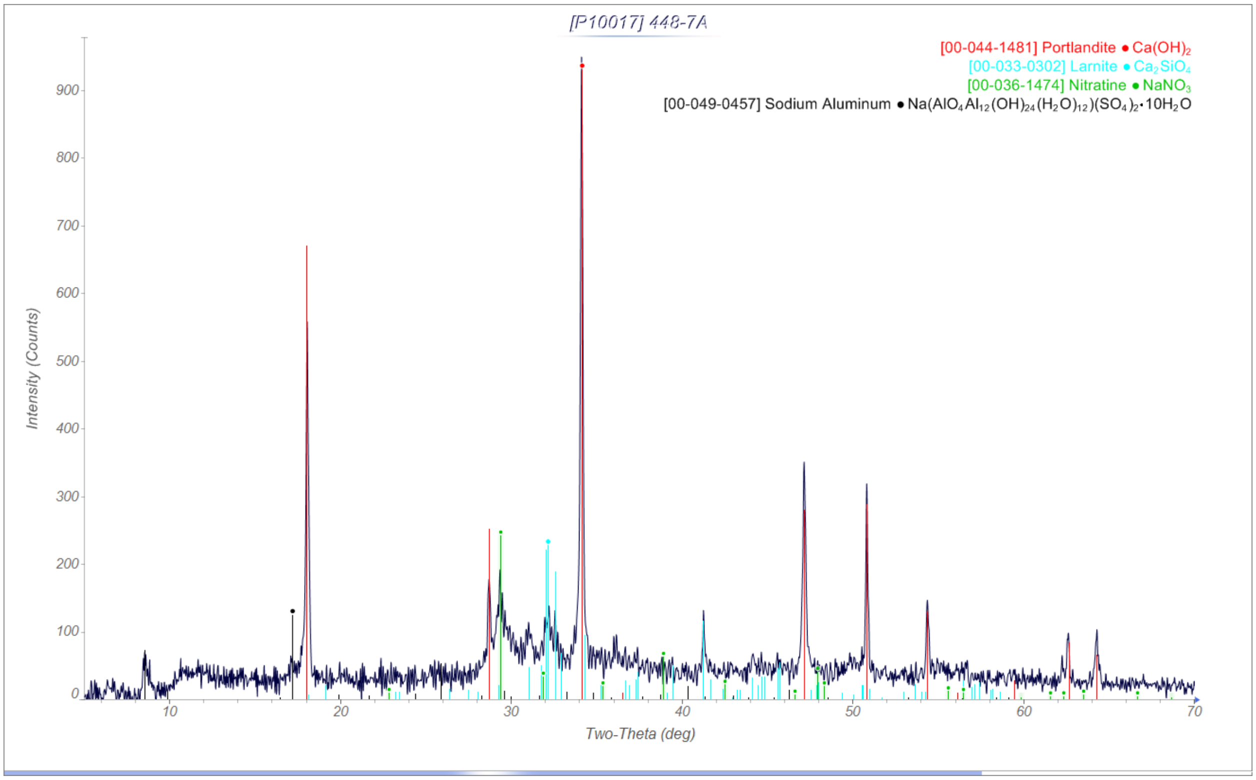
[P10017] 448-7A
[00-044-1481] Portlandite ● $Ca(OH)_2$
[00-033-0302] Larnite ● Ca_2SiO_4
[00-036-1474] Nitratine ● $NaNO_3$
[00-049-0457] Sodium Aluminum ● $Na(AlO_4Al_{12}(OH)_{24}(H_2O)_{12})(SO_4)_2 \cdot 10H_2O$
Intensity (Counts)
900
800
700
600
500
400
300
200
100
0
10
20
30
40
50
60
70
Two-Theta (deg)

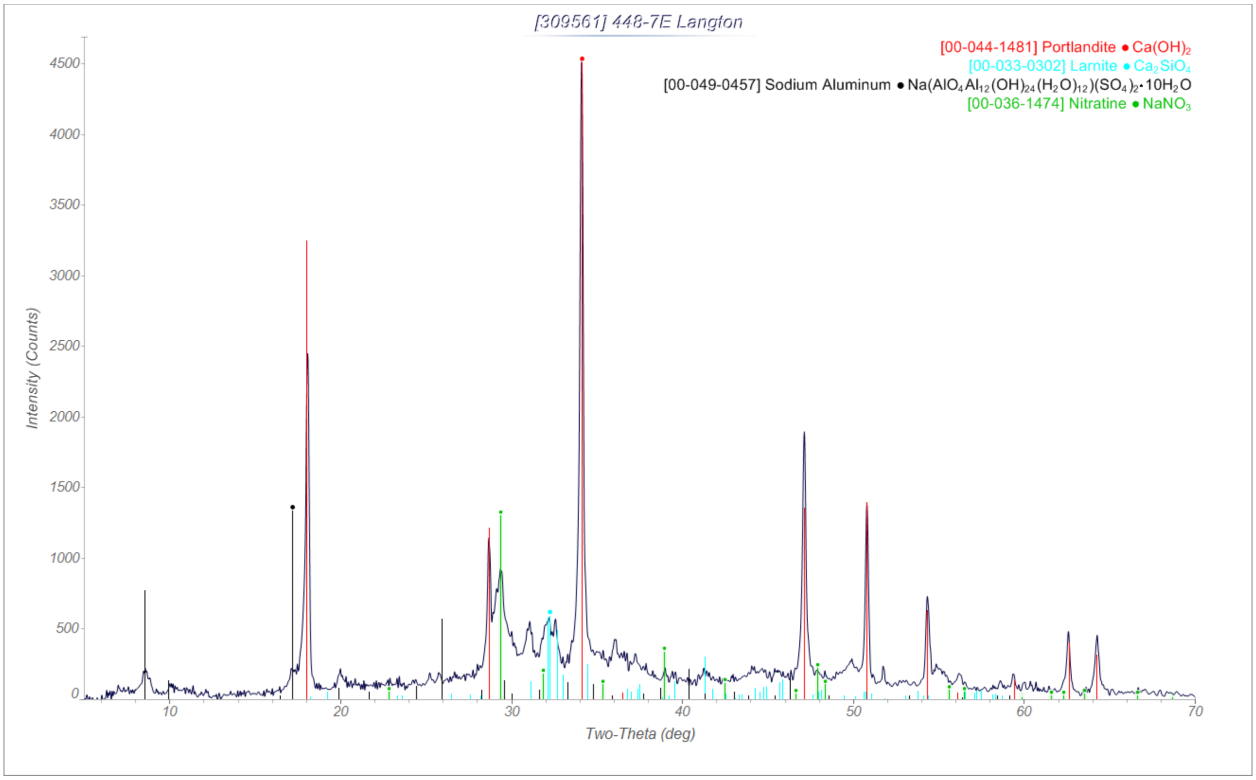
[309561] 448-7E Langton
[00-044-1481] Portlandite ● $Ca(OH)_2$
[00-033-0302] Larnite ● Ca_2SiO_4
[00-049-0457] Sodium Aluminum ● $Na(AlO_4Al_{12}(OH)_{24}(H_2O)_{12})(SO_4)_2 \cdot 10H_2O$
[00-036-1474] Nitratine ● $NaNO_3$
Intensity (Counts)
4500
4000
3500
3000
2500
2000
1500
1000
500
0
10
20
30
40
50
60
70
Two-Theta (deg)

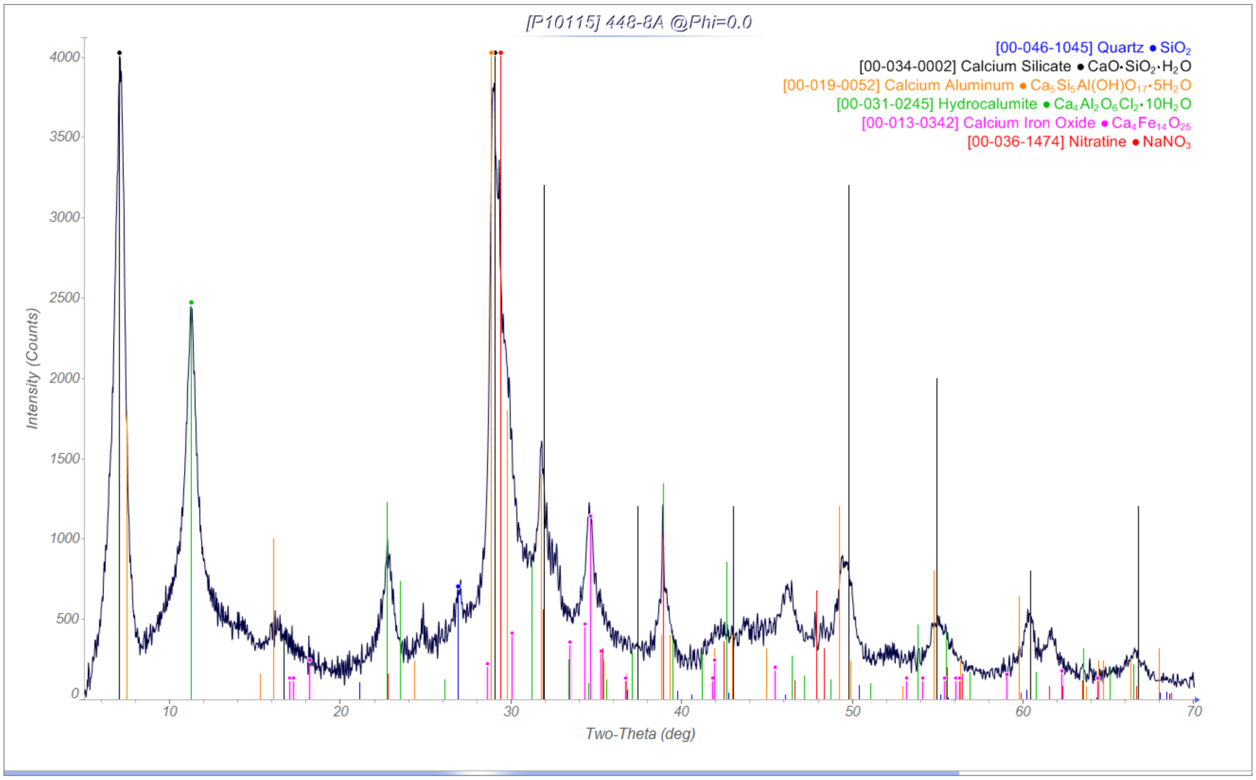
[P10115] 448-8A @Phi=0.0
[00-046-1045] Quartz ● SiO_2
[00-034-0002] Calcium Silicate ● $CaO \cdot SiO_2 \cdot H_2O$
[00-019-0052] Calcium Aluminum ● $Ca_5Si_5Al(OH)O_{17} \cdot 5H_2O$
[00-031-0245] Hydrocalumite ● $Ca_4Al_2O_6Cl_2 \cdot 10H_2O$
[00-013-0342] Calcium Iron Oxide ● $Ca_4Fe_{14}O_{25}$
[00-036-1474] Nitratine ● $NaNO_3$
Intensity (Counts)
4000
3500
3000
2500
2000
1500
1000
500
0
10
20
30
40
50
60
70
Two-Theta (deg)

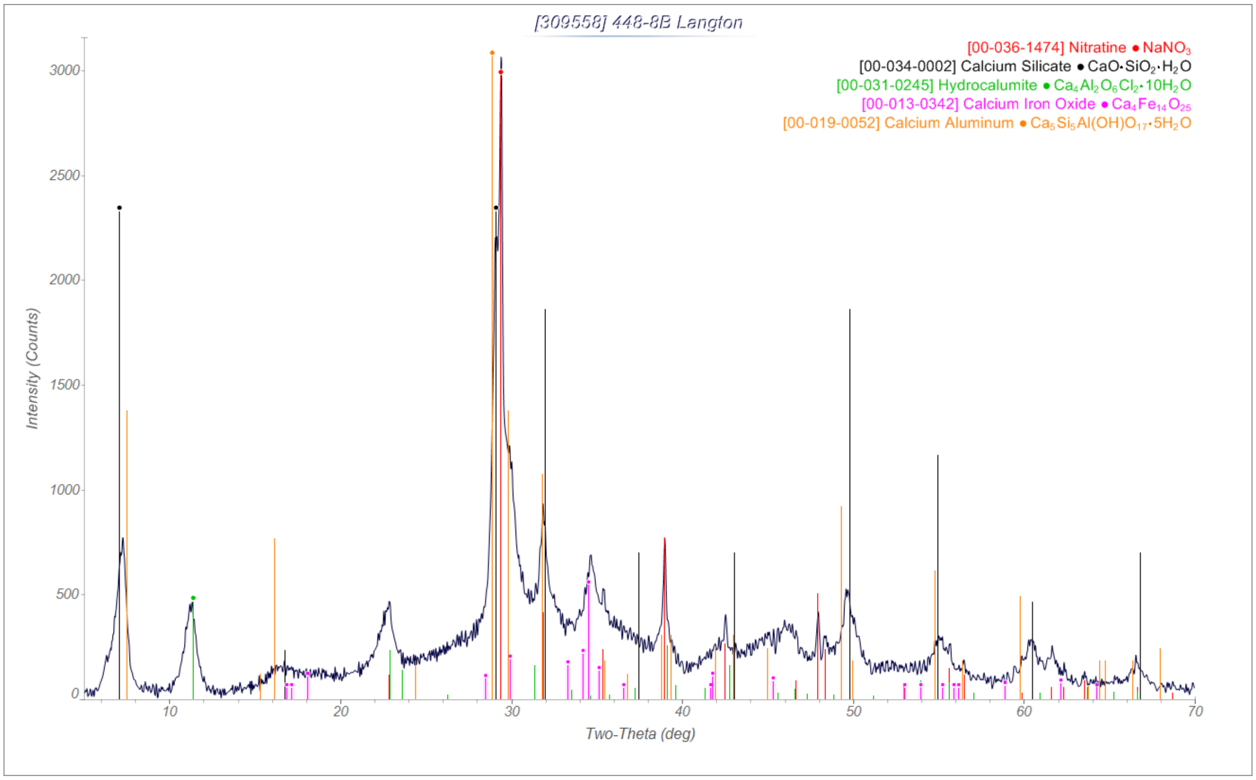
[309558] 448-8B Langton
[00-036-1474] Nitratine ● $NaNO_3$
[00-034-0002] Calcium Silicate ● $CaO \cdot SiO_2 \cdot H_2O$
[00-031-0245] Hydrocalumite ● $Ca_4Al_2O_6Cl_2 \cdot 10H_2O$
[00-013-0342] Calcium Iron Oxide ● $Ca_4Fe_{14}O_{25}$
[00-019-0052] Calcium Aluminum ● $Ca_5Si_5Al(OH)O_{17} \cdot 5H_2O$
Intensity (Counts)
3000
2500
2000
1500
1000
500
0
10
20
30
40
50
60
70
Two-Theta (deg)

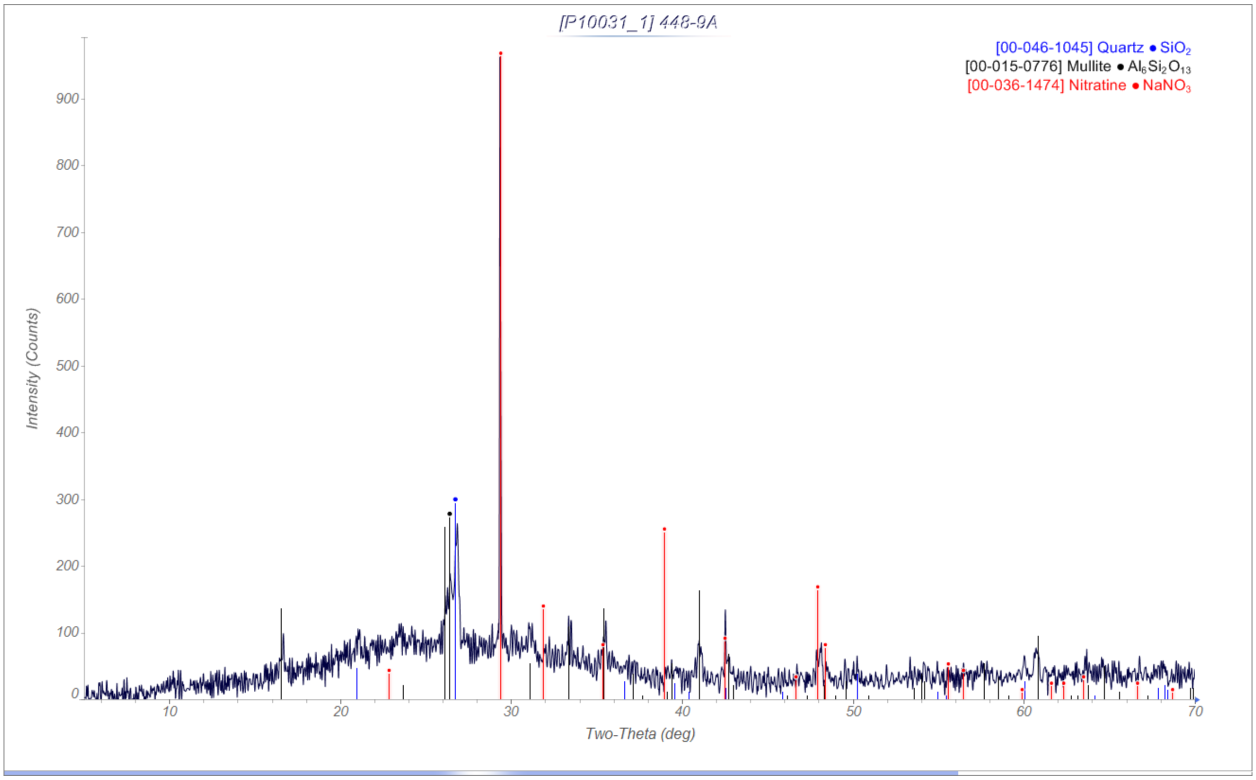
[P10031_1] 448-9A
[00-046-1045] Quartz • SiO_2
[00-015-0776] Mullite • $Al_6Si_2O_{13}$
[00-036-1474] Nitratine • $NaNO_3$
Intensity (Counts)
900
800
700
600
500
400
300
200
100
0
10
20
30
40
50
60
70
Two-Theta (deg)

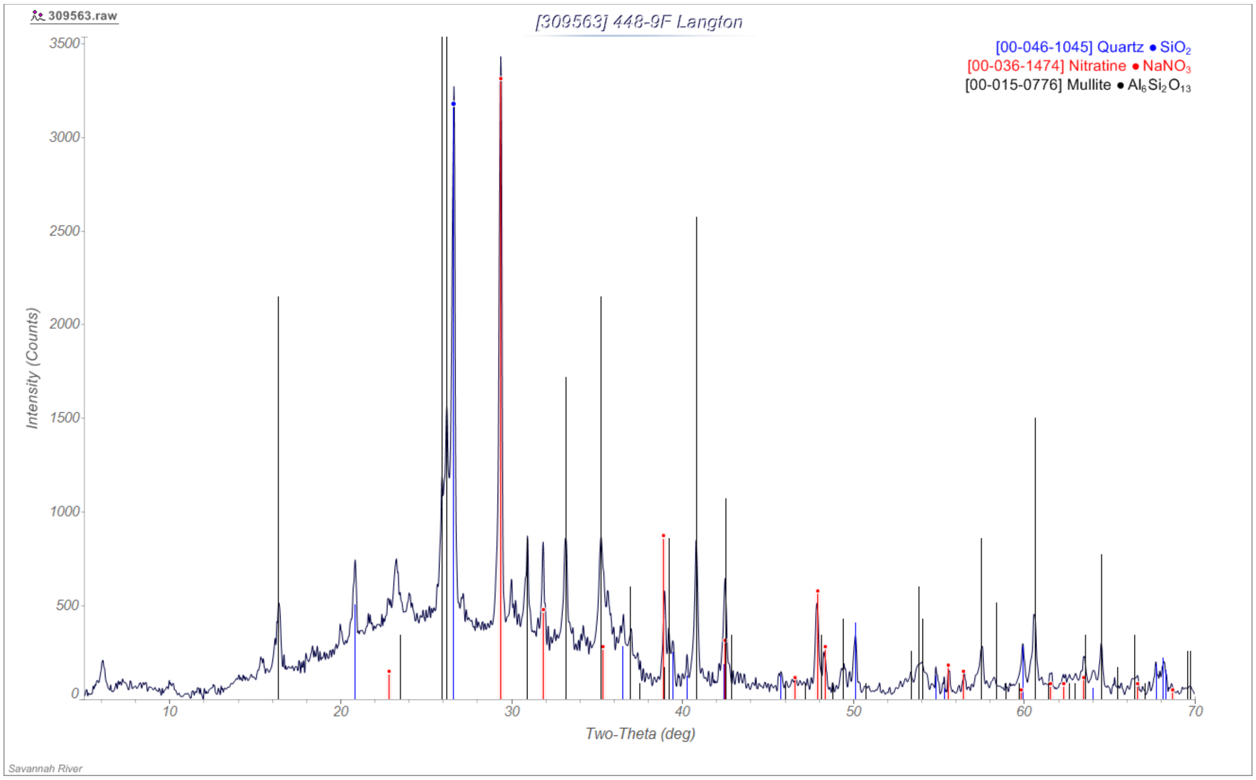
309563.raw
[309563] 448-9F Langton
[00-046-1045] Quartz • SiO_2
[00-036-1474] Nitratine • $NaNO_3$
[00-015-0776] Mullite • $Al_6Si_2O_{13}$
Intensity (Counts)
3500
3000
2500
2000
1500
1000
500
0
10
20
30
40
50
60
70
Two-Theta (deg)
Savannah River

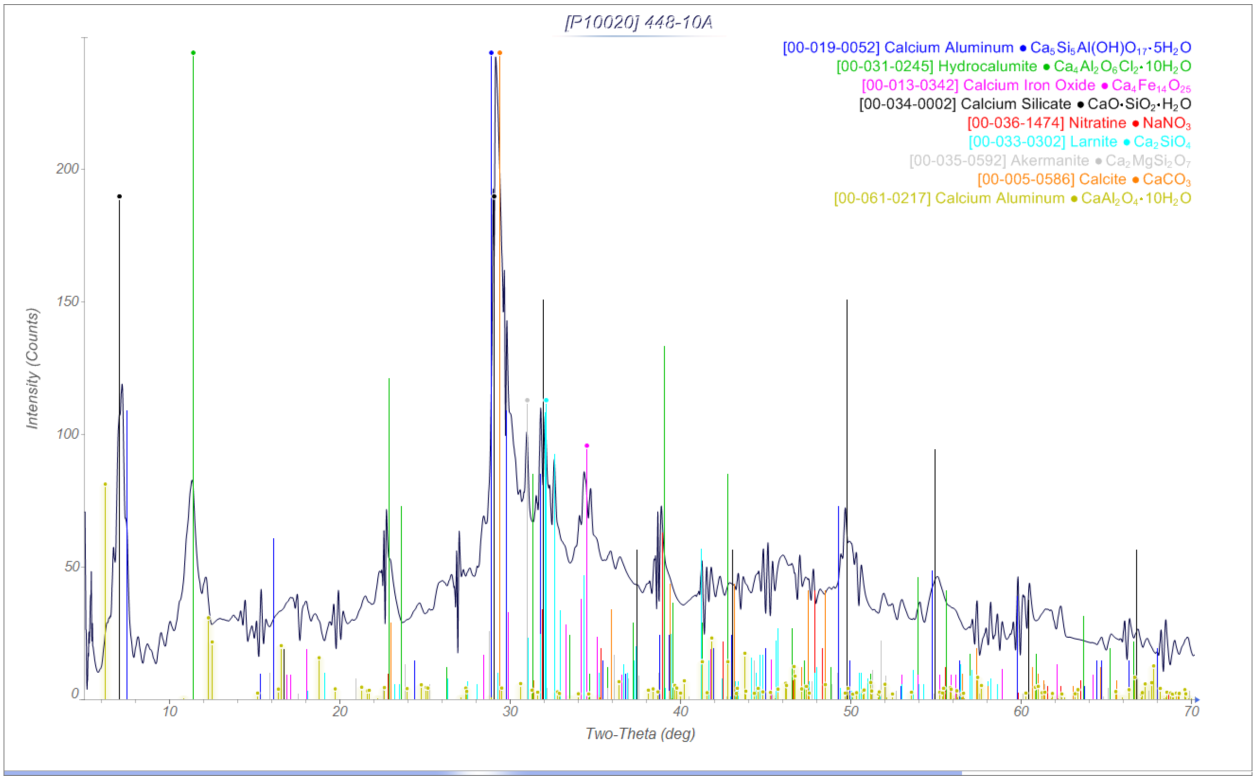
[P10020] 448-10A
[00-019-0052] Calcium Aluminum ● $Ca_5Si_5Al(OH)O_{17}\cdot 5H_2O$
[00-031-0245] Hydrocalumite ● $Ca_4Al_2O_6Cl_2\cdot 10H_2O$
[00-013-0342] Calcium Iron Oxide ● $Ca_4Fe_{14}O_{25}$
[00-034-0002] Calcium Silicate ● $CaO\cdot SiO_2\cdot H_2O$
[00-036-1474] Nitratine ● $NaNO_3$
[00-033-0302] Larnite ● Ca_2SiO_4
[00-035-0592] Akermanite ● $Ca_2MgSi_2O_7$
[00-005-0586] Calcite ● $CaCO_3$
[00-061-0217] Calcium Aluminum ● $CaAl_2O_4\cdot 10H_2O$
Intensity (Counts)
0
50
100
150
200
Two-Theta (deg)
10
20
30
40
50
60
70

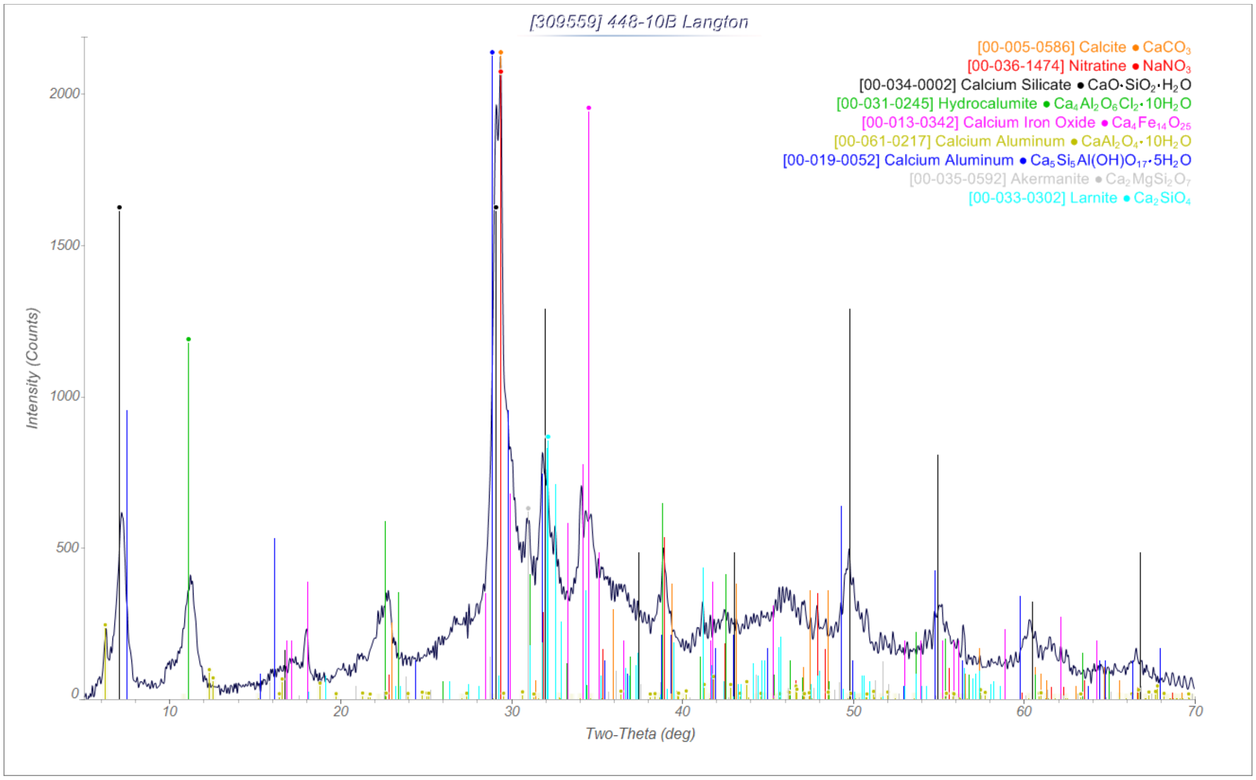
[309559] 448-10B Langton
[00-005-0586] Calcite ● $CaCO_3$
[00-036-1474] Nitratine ● $NaNO_3$
[00-034-0002] Calcium Silicate ● $CaO\cdot SiO_2\cdot H_2O$
[00-031-0245] Hydrocalumite ● $Ca_4Al_2O_6Cl_2\cdot 10H_2O$
[00-013-0342] Calcium Iron Oxide ● $Ca_4Fe_{14}O_{25}$
[00-061-0217] Calcium Aluminum ● $CaAl_2O_4\cdot 10H_2O$
[00-019-0052] Calcium Aluminum ● $Ca_5Si_5Al(OH)O_{17}\cdot 5H_2O$
[00-035-0592] Akermanite ● $Ca_2MgSi_2O_7$
[00-033-0302] Larnite ● Ca_2SiO_4
Intensity (Counts)
0
500
1000
1500
2000
Two-Theta (deg)
10
20
30
40
50
60
70

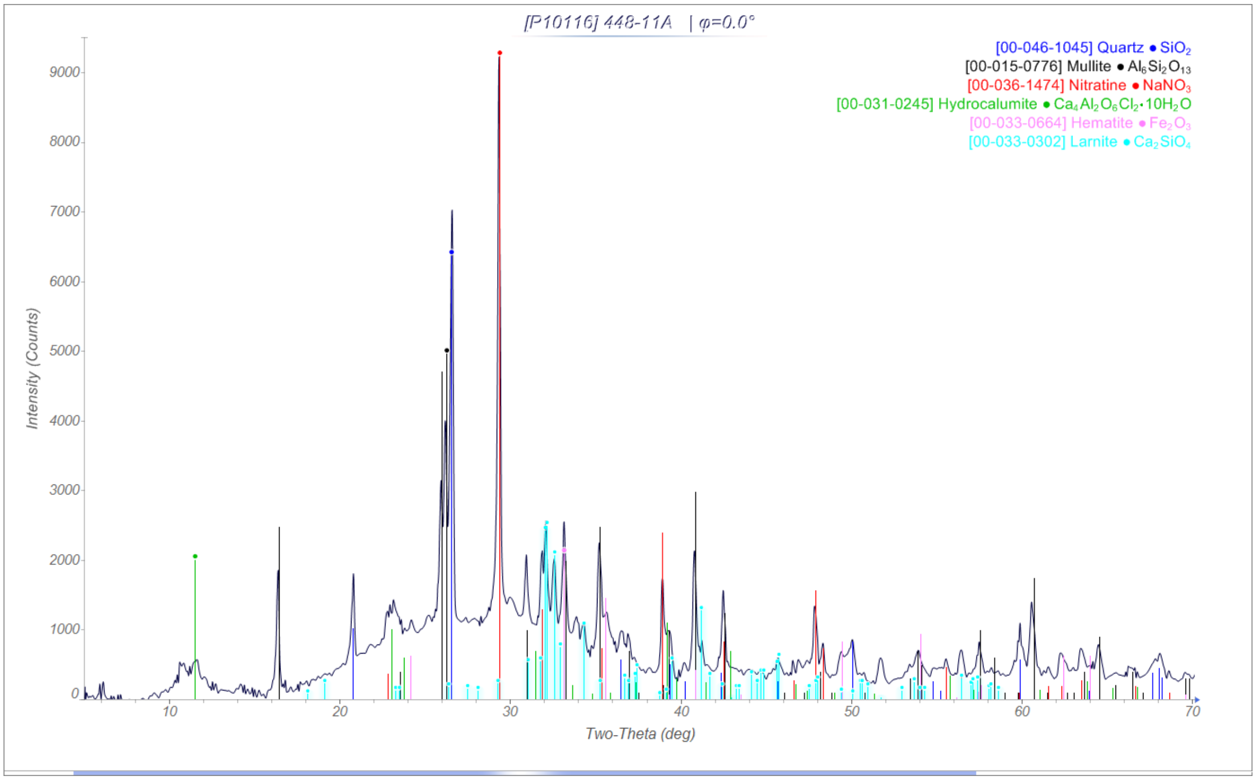
[P10116] 448-11A | φ=0.0°
[00-046-1045] Quartz ● SiO_2
[00-015-0776] Mullite ● $Al_6Si_2O_{13}$
[00-036-1474] Nitratine ● $NaNO_3$
[00-031-0245] Hydrocalumite ● $Ca_4Al_2O_6Cl_2\cdot 10H_2O$
[00-033-0664] Hematite ● Fe_2O_3
[00-033-0302] Larnite ● Ca_2SiO_4
Intensity (Counts)
0
1000
2000
3000
4000
5000
6000
7000
8000
9000
Two-Theta (deg)
10
20
30
40
50
60
70

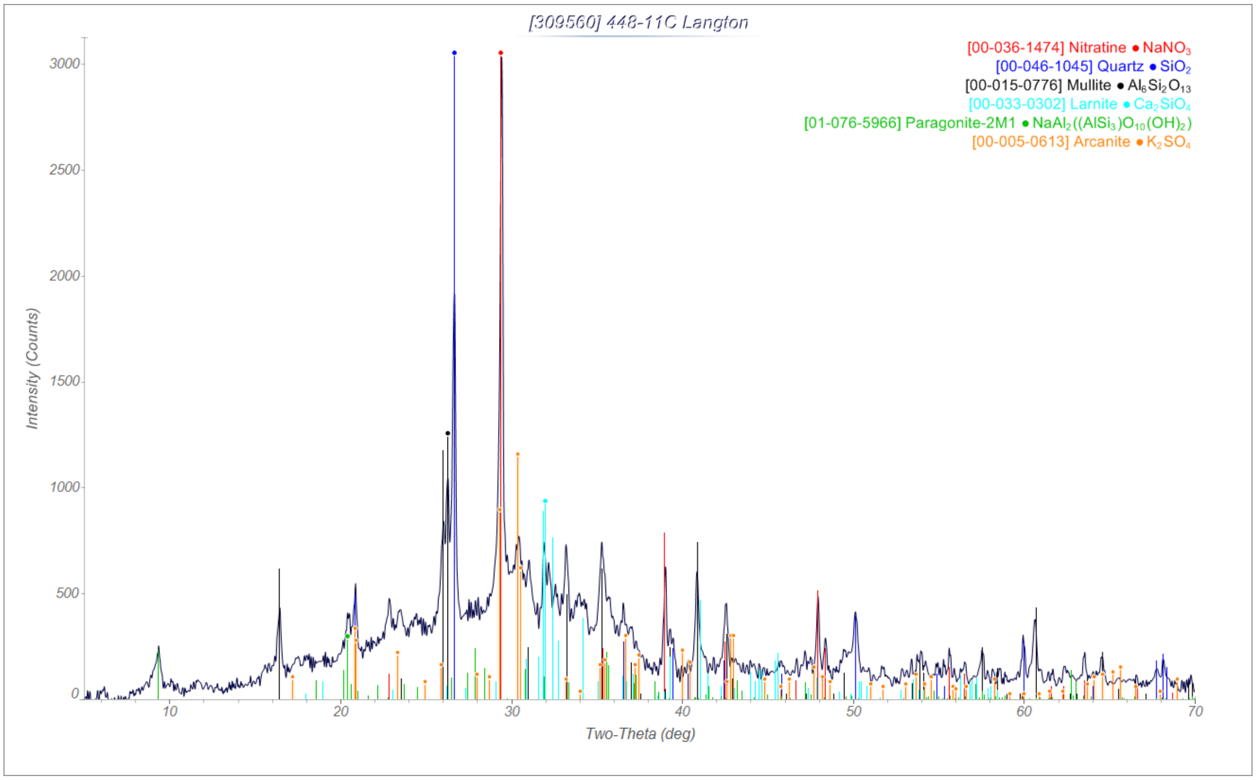
[309560] 448-11C Langton
[00-036-1474] Nitratine ● $NaNO_3$
[00-046-1045] Quartz ● SiO_2
[00-015-0776] Mullite ● $Al_6Si_2O_{13}$
[00-033-0302] Larnite ● Ca_2SiO_4
[01-076-5966] Paragonite-2M1 ● $NaAl_2((AlSi_3)O_{10}(OH)_2)$
[00-005-0613] Arcanite ● K_2SO_4
Intensity (Counts)
0
500
1000
1500
2000
2500
3000
Two-Theta (deg)
10
20
30
40
50
60
70

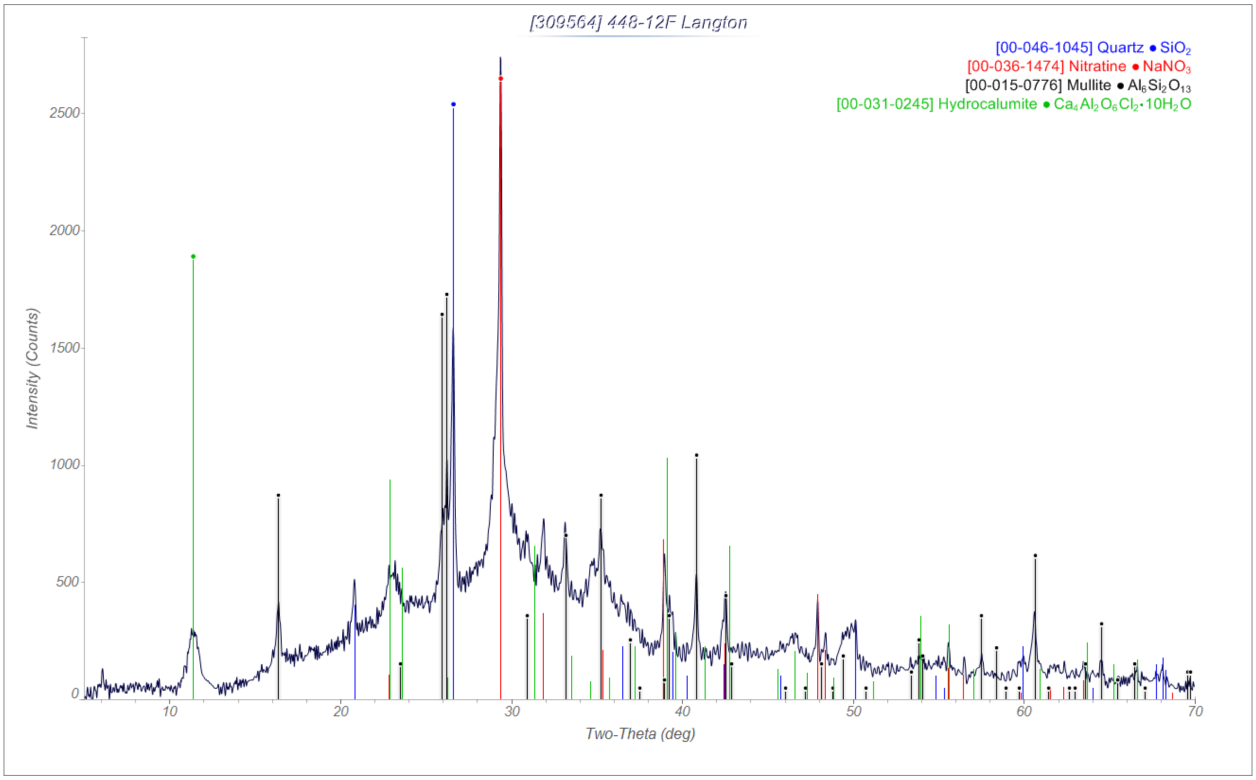
[309564] 448-12F Langton
[00-046-1045] Quartz ● SiO_2
[00-036-1474] Nitratine ● $NaNO_3$
[00-015-0776] Mullite ● $Al_6Si_2O_{13}$
[00-031-0245] Hydrocalumite ● $Ca_4Al_2O_6Cl_2 \cdot 10H_2O$
Intensity (Counts)
0
500
1000
1500
2000
2500
10
20
30
40
50
60
70
Two-Theta (deg)

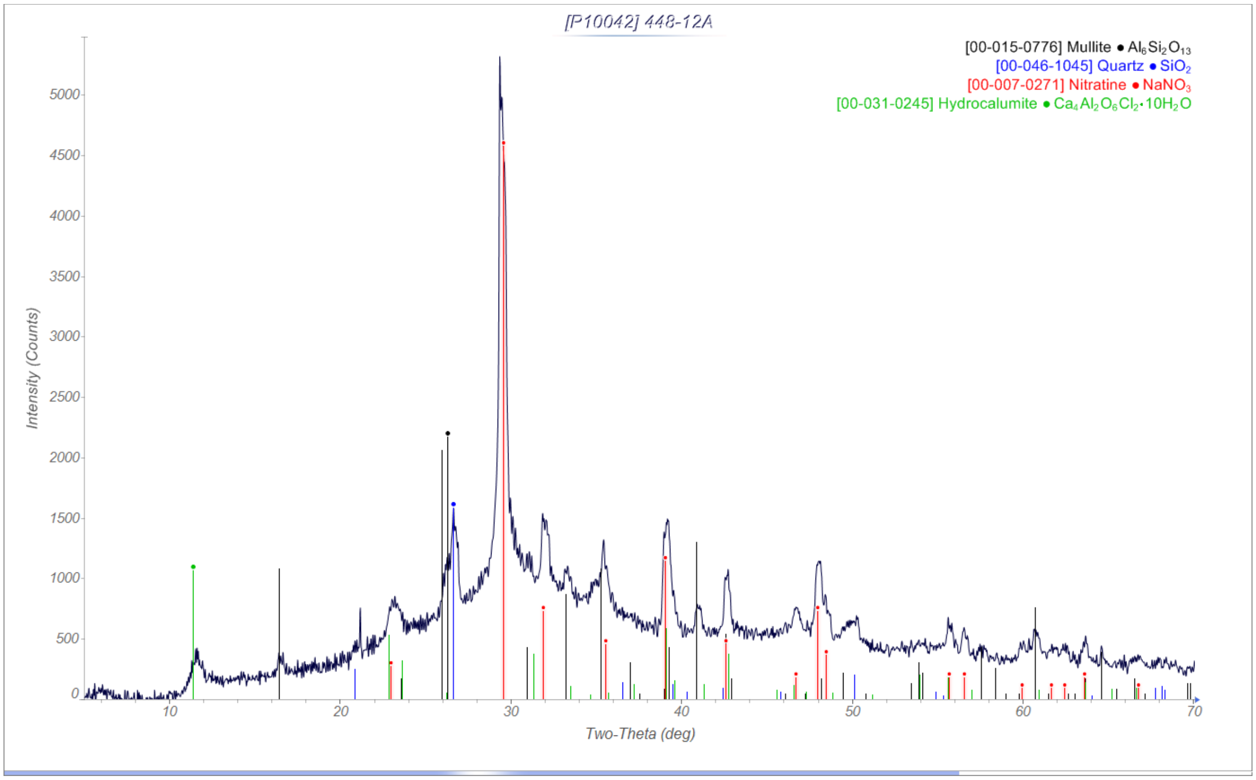
[P10042] 448-12A
[00-015-0776] Mullite ● $Al_6Si_2O_{13}$
[00-046-1045] Quartz ● SiO_2
[00-007-0271] Nitratine ● $NaNO_3$
[00-031-0245] Hydrocalumite ● $Ca_4Al_2O_6Cl_2 \cdot 10H_2O$
Intensity (Counts)
0
500
1000
1500
2000
2500
3000
3500
4000
4500
5000
10
20
30
40
50
60
70
Two-Theta (deg)

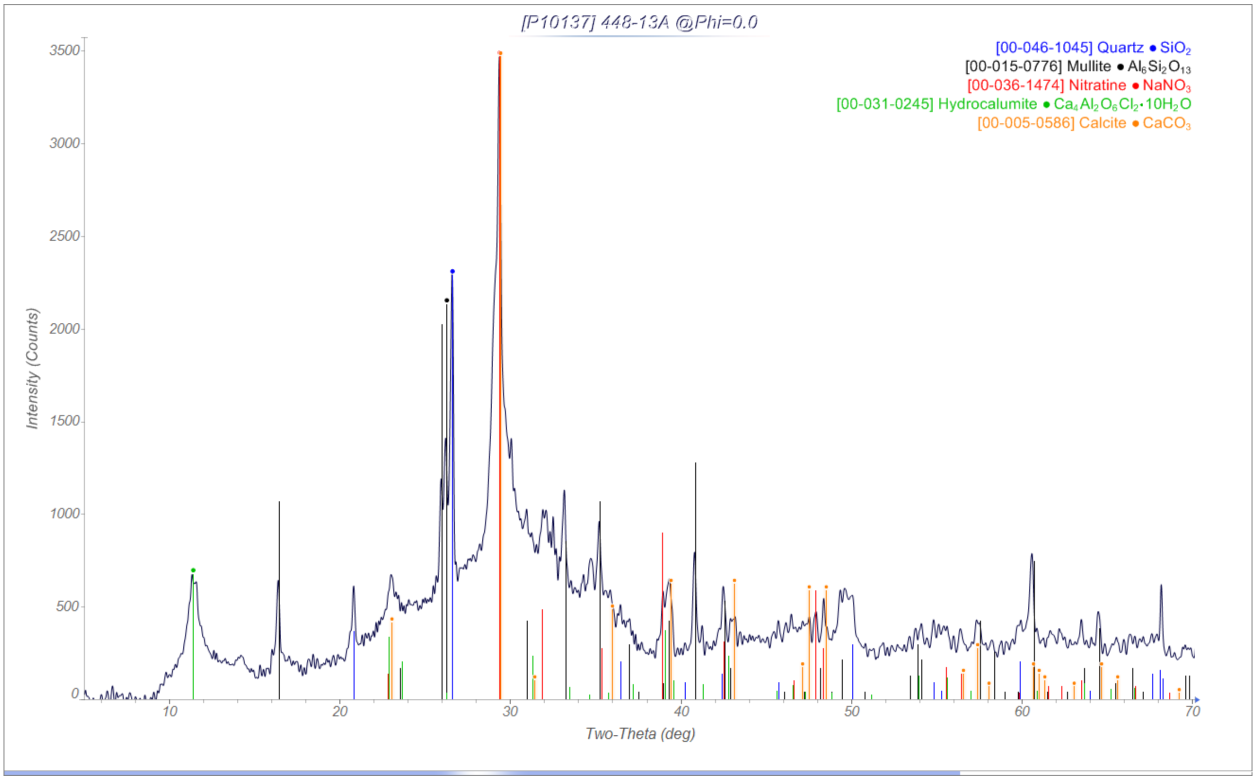
[P10137] 448-13A @Phi=0.0
[00-046-1045] Quartz • SiO_2
[00-015-0776] Mullite • $Al_6Si_2O_{13}$
[00-036-1474] Nitratine • $NaNO_3$
[00-031-0245] Hydrocalumite • $Ca_4Al_2O_6Cl_2 \cdot 10H_2O$
[00-005-0586] Calcite • $CaCO_3$
Intensity (Counts)
0
500
1000
1500
2000
2500
3000
3500
10
20
30
40
50
60
70
Two-Theta (deg)

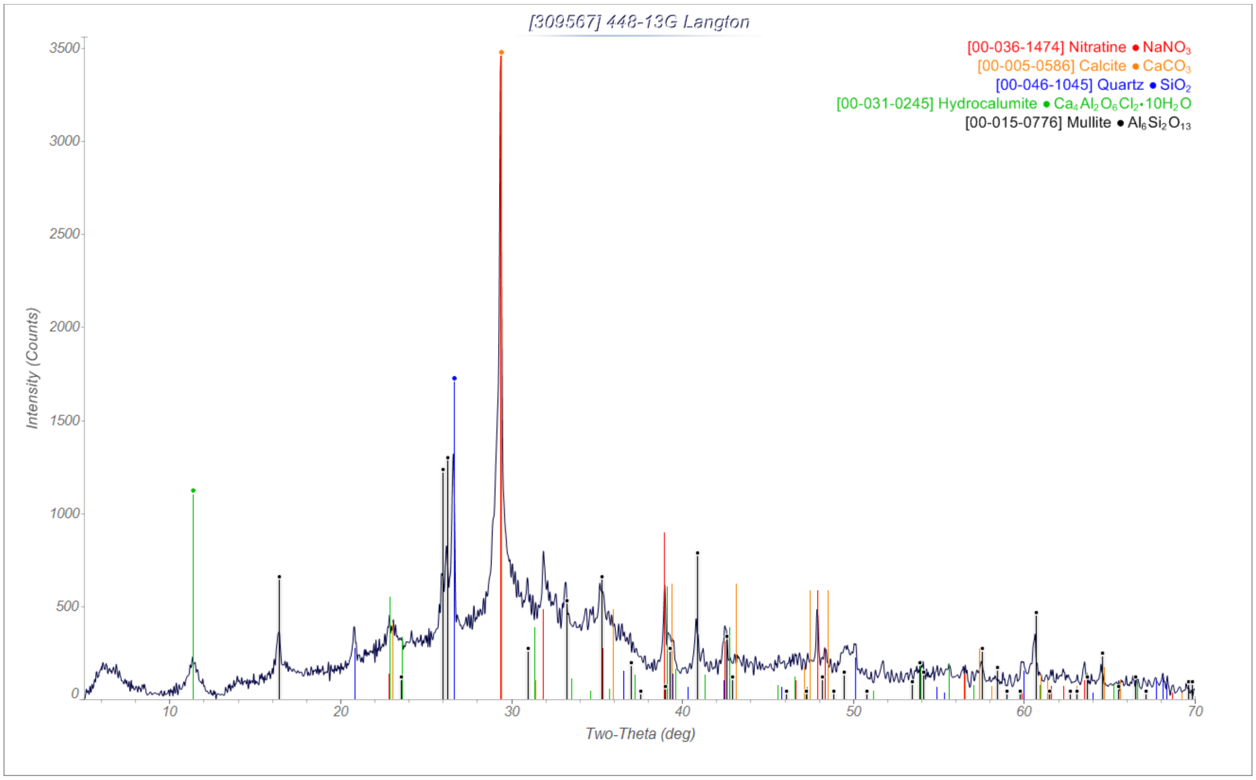
[309567] 448-13G Langton
[00-036-1474] Nitratine • $NaNO_3$
[00-005-0586] Calcite • $CaCO_3$
[00-046-1045] Quartz • SiO_2
[00-031-0245] Hydrocalumite • $Ca_4Al_2O_6Cl_2 \cdot 10H_2O$
[00-015-0776] Mullite • $Al_6Si_2O_{13}$
Intensity (Counts)
0
500
1000
1500
2000
2500
3000
3500
10
20
30
40
50
60
70
Two-Theta (deg)